Informe Productividad 2020 DIE-UC

TABLA DE CONTENIDO

INTRODUCCION

Durante el año 2020, el Departamento de Ingeniería Eléctrica de la Pontificia Universidad Católica de Chile, pese a la contingencia mundial provocada por la pandemia del COVID 19, ha continuado con su labor de investigación a través de estudios publicados en revistas, tesis y el desarrollo de proyectos financiados por Fondecyt, Fondef y otras fuentes en las diferentes especialidades de la Ingeniería Eléctrica.

El presente Informe reúne lo publicado por los profesores e investigadores de nuestro Departamento en sus distintas especialidades y tiene por objetivo dar a conocer en forma más detallada el trabajo de investigación realizado durante el año 2020. Cabe destacar que nuestro año académico fue completamente online, por lo que muchas de las actividades internas y de difusión de nuestro quehacer se vieron mermadas a raíz de la pandemia que aún nos afecta.

El Informe incluye los siguientes contenidos:

- Tesistas graduados del Programa de Doctorado en Ciencias de la Ingeniería.
- Tesistas graduados del Programa de Magister en Ciencias de la Ingeniería.
- Publicaciones en revistas ISI.
- Proyectos de investigación desarrollados.
- Actividades internas y difusión.

INDICES DE PRODUCTIVIDAD AÑO 2020

PHD. CIENCIAS DE LA INGENIERÍA	**1**
MAGISTER EN CIENCIAS DE INGENIERÍA	**8**
TITULADOS DE INGENIERÍA ELÉCTRICA	**42**
PUBLICACIONES ISI	**5** **5**
PROYECTOS DE INVESTIGACIÓN	**2** **3**

I. TESISTAS GRADUADOS DEL PROGRAMA DE DOCTORADO EN CIENCIAS DE LA INGENIERIA

Tesista: Aline Carvalho da Silva Xavier
Tesis: ¨Fatty acids characterization during non- alcoholic fatty liver disease using magnetic resonance spectroscopy¨.
Supervisor: Marcelo Andía
Fecha de la defensa: 22/07/2020

Resumen: La enfermedad del hígado graso no-alcohólico (EHGNA) es la enfermedad hepática más común en el mundo y el único método disponible para determinar de manera confiable su etapa esteatosis, esteatohepatitis, fibrosis o cirrosis) es la biopsia hepática, la cual es invasiva y riesgosa para los pacientes. El objetivo de esta tesis es investigar la composición de los ácidos grasos hepáticos durante la progresión de laEHGNA mediante el uso de espectroscopía por resonancia magnética (ERM), buscando encontrar una manera de clasificar las etapas de esta enfermedad de manera no-invasiva. Para esto, realizamos estudios invivo y ex-vivo en modelos animales de EHGNA. Además, demostramos la viabilidad de aplicar nuestras técnicas en humanos. Nuestros resultados mostraron que la composición de los ácidos grasos hepáticos cambia a medida que laEHGNA progresa de esteatosis a esteatohepatitis, donde alcanzan un pleateau y permanece invariabledurante la progresión de la esteatohepatitis. Utilizandoanálisis de componentes principales fue posible identificar los tres grupos clínicos más relevantes: normal, esteatosis y esteatohepatitis. En esta tesis se demostró que es posible detectar la progresión de la esteatosis simple a esteatohepatitis utilizando ERM hepática y que este método tiene lafactibilidad de ser utilizado en la clínica.

II. TESISTAS GRADUADOS DEL PROGRAMA DE MAGISTER EN CIENCIAS DE LA INGENIERIA

Tesista: Juan Andrés Bozzo Jiménez
Tesis: "A blind calibration scheme for switched-capacitor pipeline analog-to-digital converters".
Supervisor: Ángel Abusleme
Fecha de la defensa: 05/03/2020
Resumen: Se presenta un nuevo esquema de calibración foreground para conversores de datos análogo-a-digital (ADC), diseñado para auto-calibrar un ADC pipeline de capacitores conmutados. La calibración estima parámetros eléctricos del ADC; capacitores, referencias de voltaje y pérdida de carga debido a ganancia finita. La estimación es usada para compensar digitalmente errores de conversión durante la operación normal del ADC. El algoritmo de calibración se basa en la instanciación de conversores ΔΣ en la interfaz entre etapas pipeline reorganizando los componentes eléctricos de las etapas pipeline. Diferentes configuraciones pueden ser probadas usando señales de entrada auto-generadas, lo que permite al algoritmo inferir los parámetros eléctricos subyacentes. La calibración es realizada por la misma circuitería que opera durante el funcionamiento normal del conversor y no requiere de un circuito o voltage que actúe como tierra real. Sin embargo depende de los voltajes the threshold de los sub-ADCs de las etapas pipeline, haciéndolo inadecuado para ciruitos donde el error de los sub-ADCs es dominante. El comportamiento de un número de ADCs de 10 bits con una ENOB de 6.3 bits fué simulado y una mejora en resolución entre 2.5 bits para el mejor caso y 1 bit para el peor fué observada.

Tesista: Martín Eduardo Calvo Sánchez
Tesis: "Online Inertial Parameter Estimation For Robotic Loaders".
Supervisor: Miguel Torres
Fecha de la defensa: 27/07/2020
Resumen: La masa transportada, roce viscoso y centro de masa de cargadores y maquinarias movedoras de tierra son fundamentales para monitorear productividad, y otros aspectos como planificación de operaciones y mantenimiento. La masa de la carga se ha medido típicamente usando sensores de galga extensométrica. Sin embargo, estos sensores requieren frecuentes re-calibraciones debido a estrés mecánico y no entregan información sobre roce viscoso. Este trabajo presenta un método básado en un observador para estimar en línea la masa de un cargador, su inercia rotacional, centro de masa y coeficientes de roce viscoso usando mediciones de torque, velocidad y aceleración. Un aspecto novedoso es la introducción de un criterio de información mutua, para seleccionar datos que aseguren una identificación adecuada de los parámetros, en adición a la aplicación de excitaciones apropiadas al sistema. El método se compara con estimaciones de mínimos cuadrados y sus variantes: recursivo, generalizado factible y totales. El método propuesto es validado en simulación y en experimentos usando una minicargadora industrial Cat®262C. La masa es estimada con un error RMS bajo el 1% del total. Movimientos rotacionales y complejos también fueron probados para evaluar la factibilidad de obtener la inercia rotacional, centro de masa y parámetros de roce.

Tesista: Felipe Antonio Chaparro Pérez
Tesis: "Implementing a power hardware in-the-loop platform using the damping impedance method".
Supervisor: Javier Pereda
Fecha de la defensa: 08/10/2020

Resumen: El testeo y la validación son partes esenciales del desarrollo de cualquier dispositivo eléctrico de potencia. Las simulaciones Power Hardware in-the-loop pueden desempeñar un papel vital en la mejora de la fase de prueba de estos dispositivos, permitiendo escenarios de prueba realistas y, reducir costes, riesgos y ahorrar tiempo.
Esta tesis presenta un trabajo de investigación sobre la implementación práctica de una plataforma de simulación PHIL utilizando el Damping Impedance Method. Para tener éxito, esto requiere la identificación de la impedancia del dispositivo bajo prueba. Presentamos una estrategia de identificación basada en el análisis espectral, para obtener una identificación no paramétrica de la impedancia del HUT, seguida de una rutina de ajuste que obtiene una representación paramétrica de la misma. A continuación, se simula la plataforma PHIL para probar su funcionamiento, así como el de la rutina de identificación con HUT pasivos y activos. La implementación de la plataforma PHIL se realiza en un simulador multinúcleo de tiempo real, lo que permite que la simulación eléctrica y la rutina de identificación se ejecuten en paralelo, en un mismo dispositivo. Se realiza luego, una verificación experimental de los escenarios simulados. Se encuentra una diferencia fundamental entre la identificación de los HUT pasivos y activos y se proponen y aplican estrategias sobre cómo hacer frente a ella. Finalmente, se dan recomendaciones sobre la realización de más simulaciones PHIL con la plataforma.

Tesista: Rodrigo Hernán Cuzmar Leiva
Tesis: "Predictive Control of Cascaded H-Bridge converters under interphase and intercell unbalanced solar power generation".
Supervisor: Javier Pereda
Fecha de la defensa: 11/03/2020

Resumen: Actualmente, el mundo está en un proceso de transición en la forma de generar energía, desde una matriz energética basada en recursos fósiles a una basada en energías renovables. Dentro de las energías renovables, una de las que destaca es la energía solar. Sin embargo, los sistemas solares fotovoltaicos (PV) presentan desafíos, por ejemplo, sombra parcial, suciedad, irradiación no uniforme, límite de voltaje y falta de modularidad, problemas que producen desequilibrios en la generación y reducen la eficiencia y la confiabilidad del sistema. Esta investigación propone el desarrollo de un método predictivo no invasivo para el control de un conversor CHB para una correcta inyección de potencia a la red bajo una generación desbalanceada, reduciendo distorsión armónica y voltaje de modo común. De esta manera, se realizan simulaciones del sistema para determinar el desempeño de la propuesta. Además, se prueba la propuesta en un prototipo experimental para verificar su funcionamiento. Finalmente, los resultados obtenidos comprueban la capacidad de la estrategia de control para inyectar potencia balanceada a partir de una generación desbalanceada entre fases y celdas. Adicionalmente, la propuesta mantiene un voltaje de modo común en torno a cero y un bajo esfuerzo computacional.

Tesista: Gabriel Emilio Durán Godoy
Tesis: "Computer System for Harmonic Transcription of Jazz Music".
Supervisor: Patricio De La Cuadra
Fecha de la defensa: 14/08/2020
Resumen: La transcripción automática de acordes es un tema ampliamente estudiado por la comunidad científica, que presenta un problema complejo puesto que es un concepto musical estrechamente relacionado a la percepción humana. En los últimos años se han logrado sustanciales avances utilizando métodos de aprendizaje profundo, sin embargo la mayoría de éstos estudios se han desarrollado sobre géneros musicales como el pop o el rock, no siendo generalizables a la música de jazz, cuya naturaleza fuertemente improvisada causa que no se cumplan muchos de los supuestos sobre cómo se percibe la armonía. En esta investigación se presenta un sistema computacional para realizar transcripción de acordes en canciones de jazz, abordando los desafíos específicos que éstas presentan e incorporando al análisis elementos musicales propios del género. Esto se logra realizando un estudio detallado de subproblemas, que nos permite tener un mejor entendimiento de cómo se debe adaptar los métodos estándar sobre este género musical, para así integrar diferentes elementos musicales en el análisis. Este sistema es capaz de obtener una representación de acordes del tipo "hoja guía" a partir del audio. El primer subproblema abordado es la detección de cambios de notas del bajo, puesto que éstos están estrechamente relacionados con cambios de acordes. Luego, se estudia la sincronización musical para lograr alinear los diferentes segmentos repetidos de una canción y analizar el contenido musical de cada uno de ellos. Por último se implementa el sistema de transcripción de acordes utilizando una red neuronal convolucional recurrente, que logra obtener en conjunto la secuencia de acordes y el pulso. Esta metodología de transcripción de acordes logra un 71% de precisión bajo la métrica de desempeño MIREX, que es mayor que los sistemas estado del arte para la base de datos JAAH. Adicionalmente, tiene la ventaja que logra transcribir acordes y detectar el pulso en conjunto.

Tesista: Constanza Gabriela Levicán Torres
Tesis: "Metodología para el desarrollo de proyectos de microredes conectadas a la Red de Distribución en municipalidades de Chile".
Supervisor: Álvaro Lorca
Fecha de la defensa: 22/12/2020
Resumen: En esta investigación se estudia el rol de las microredes conectadas a la Red de Distribución, los beneficios que entregan al Sistema Eléctrico: calidad de servicio, confiabilidad y resiliencia, flexibilidad, los nuevos modelos de negocios que permitirán: agregadores de demanda, plantas solares virtuales, energía como servicio, prepago, proyectos energéticos comunitarios, transacciones peer-to-peer y operadores de sistemas distribuidos. Se propone una metodología para implementar proyectos pilotos en municipalidades de Chile- En la metodología se explica el cálculo de demanda energética en edificios de oficinas, perfiles de demanda, funcionamiento de las baterías y modelos de gestión de activos. Como caso de estudio, se entregan propuestas de diseño para un proyecto piloto en una municipalidad chilena, para lo cual se estudia el contexto del proyecto, la visión de la Empresa Distribuidora (Enel Distribución Chile) y el municipio (Ilustre Municipalidad de Renca). Finalmente, se realiza una evaluación económica de las configuraciones propuestas y escenarios propuestos, una sensibilización de parámetros, y finalmente, una discusión sobre los aspectos de la regulación actual que se podrían mejorar para impulsar proyectos de microredes.

Tesista: Francis Helena Martínez Firgau
Tesis: "Cutting Down Residential PV Solar Systems Prices Through Different Business Models: A Review of PV SolarSystems Cost to Discover The Real Cost That Redidential Customers Face".
Supervisor: David Watts
Fecha de la defensa: 30/06/2020
Resumen: Los sistemas solares fotovoltaicos de pequeña escala usualmente no son rentables para elsector residencial debido a los altos precios que estos implican, influenciados por la limitación o falta de información, altos costos blandos ineficientes, poca transparencia de precios y la presencia competencia monopolística en el mercado. A través del modelo econométrico de costos de sistemas solar fotovoltaicos desarrollado enesta investigación, se puede confirmar que los costos blandos representan hasta 60% del costo total de un sistema de pequeña escala y alrededor del 30% de estos son evitables. Además, sedemuestra que es posible evitar hasta 1500 USD/kW si se aprovechan las economías de escala y que a través de modelos de negocio también es posible reducir las barreras a las que se enfrentan el sector residencial, como las económicas, financieras, regulatorias, técnicas, geográficas y socioculturales. Para reducir los precios de sistemas solares fotovoltaicos a pequeña escala e incentivar sudesarrollo, se propone recopilar y analizar información de costos para proporcionar transparencia de precios al sector público y permitir la competencia en el mercado; desarrollar modelos de negocio basados en la compra agregada para reducir hasta un 300% el costo inicial y aprovechar las bajas tasas de interés como las tasas hipotecarias para disminuir las barreras financieras. Revista científica catalogada ISI (Web of Science) al cuál fue enviado el artículo: Renewable & Sustainable Energy Reviews.

Tesista: Gabriel Matías Yuseff Campusano
Tesis: "Stability Analysis of Distribution Network with Distributed Generation and Soft-Open-Point".
Supervisor: Javier Pereda
Fecha de la defensa: 17/01/2020
Resumen: La red de distribución está viviendo la transformación más grande de la historia, la cual es empujada por la aparición de la generación distribuida y la electro movilidad, estas ya están causando gran presión sobre las ciudades que poseen estas tecnologías. Una de las soluciones que se están analizando es un mayor control de la red por medio de la electrónica de potencia, ya sean trabajando en las subestaciones o conectadas en puntos claves de la red. Una de estas soluciones son los Soft-Open-Point, en donde se conectan dos nodos por medio de un conversor, permitiendo un manejo en el traspaso de potencia entre estos puntos. Esta investigación se enfoca en el impacto que tiene esta tecnología en la estabilidad de una red de distribución la cual también presenta una fuente de generación distribuida. Para ello se presentara un modelo en pequeña señal del sistema y un análisis de estabilidad basado en factores de participación y el lugar geométrico de las raíces.

III. PUBLICACIONES EN REVISTAS ISI

ANGEL ABUSLEME

A. Abusleme, (et al.) (2020)
Optimization of the JUNO liquid scintillator composition using a Daya Bay antineutrino detector.
Revista: Nuclear Instruments and Methods in Physics Research Section A: Accelerators, Spectrometers, Detectors and Associated Equipment. Volume 988, 1 February 2021, 164823
Abstract: To maximize the light yield of the liquid scintillator (LS) for the Jiangmen Underground Neutrino Observatory (JUNO), a 20 t LS sample was produced in a pilot plant at Daya Bay. The optical properties of the new LS in various compositions were studied by replacing the gadolinium-loaded LS in one antineutrino detector. The concentrations of the fluor, PPO, and the wavelength shifter, bis-MSB, were increased in 12 steps from 0.5 g/L and 0.01 mg/L to 4 g/L and 13 mg/L, respectively. The numbers of total detected photoelectrons suggest that, with the optically purified solvent, the bis-MSB concentration does not need to be more than 4 mg/L. To bridge the one order of magnitude in the detector size difference between Daya Bay and JUNO, the Daya Bay data were used to tune the parameters of a newly developed optical model. Then, the model and tuned parameters were used in the JUNO simulation. This enabled to determine the optimal composition for the JUNO LS: purified solvent LAB with 2.5 g/L PPO, and 1 to 4 mg/L bis-MSB.

D. E. Hurtado, J. A. P. Chávez, R. Mansilla, R. Lopez and A. Abusleme, (2020)
"Respiratory Volume Monitoring: A Machine-Learning Approach to the Non-Invasive Prediction of Tidal Volume and Minute Ventilation.
Revista: IEEE Access, vol. 8, pp. 227936-227944
Abstract: Continuous monitoring of ventilatory parameters such as tidal volume (TV) and minute ventilation (MV) has shown to be effective in the prevention of respiratory compromise events in hospitalized patients. However, the non-invasive estimation of respiratory volume in non-intubated patients remains an outstanding challenge. In this work, we present a novel approach to respiratory volume monitoring (RVM) that continuously predicts TV and MV in normal subjects. Respiratory flow in 19 volunteers under spontaneous breathing was recorded using respiratory inductance plethysmography and a temperature-based wearable sensor. Temperature signals were processed to identify features such as temperature amplitude and mean value, among others. The feature datasets were then used to train and validate three machine-learning (ML) algorithms for the prediction of respiratory volume based on temperature-related features. A model based on Random-Forest regression resulted in the lowest root mean-square error and was subsequently chosen to predict ventilatory parameters on subject test data not used in the construction of the model. Our predictions achieve a bias (mean error) in TV and MV of 16.04 mL and 0.19 L/min, respectively, which compare well with performance metrics reported in commercially-available RVM systems based on electrical impedance. Our results show that the combination of novel respiratory temperature sensors and machine-learning algorithms can deliver accurate and continuous estimates of TV and MV in healthy subjects.

ALDO CIPRIANO

Juan s. Gómez, José Rodriguez, Cristian García, Luca Tarisciotti, Freddy Flores-Bahamonde, Javier Pereda, Felipe Núñez, Aldo Cipriano, Juan Carlos Salas (2020)
An Overview of Microgrids Challenges in the Mining Industry.
Revista: IEEE Access, vol. 8, pp. 191378-191393
Abstract: The transition from fossil fuels to renewable energies as power sources in the heavy industries is one of the main climate change mitigation strategies. The carbon footprint in mining is related to its inherent extraction process, its high demand of electric power and water, and the use of diesel. However, considering its particular power requirements, the integration of microgrids throughout the whole control hierarchy of mining industry is an emergent topic. This paper provides an overview of the opportunities and challenges derived from the synergy between microgrids and the mining industry. Bidirectional and optimal power flow, as well as the integration of power quality have been identified as microgrid features that could potentially enhance mining processes. Recommendations pertaining to the technological transition and the improvement of energy issues in mining environments are also highlighted in this work.

PABLO IRARRÁZAVAL

Milovic C., Prieto C., Bilgic B., Uribe S., Acosta-Cabronero J., Irarrazaval P., Tejos C. (2020)
Comparison of parameter optimization methods for quantitative susceptibility mapping.
Revista: Magnetic Resonance in Medicine Volume85, Issue1, January 2021. pp 480-494
Abstract: Purpose: Quantitative Susceptibility Mapping (QSM) is usually performed by minimizing a functional with data fidelity and regularization terms. A weighting parameter controls the balance between these terms. There is a need for techniques to find the proper balance that avoids artifact propagation and loss of details. Finding the point of maximum curvature in the L-curve is a popular choice, although it is slow, often unreliable when using variational penalties, and has a tendency to yield overregularized results.
Methods: We propose 2 alternative approaches to control the balance between the data fidelity and regularization terms: 1) searching for an inflection point in the log-log domain of the L-curve, and 2) comparing frequency components of QSM reconstructions. We compare these methods against the conventional L-curve and U-curve approaches.
Results: Our methods achieve predicted parameters that are better correlated with RMS error, high-frequency error norm, and structural similarity metric-based parameter optimizations than those obtained with traditional methods. The inflection point yields less overregularization and lower errors than traditional alternatives. The frequency analysis yields more visually appealing results, although with larger RMS error.
Conclusion: Our methods provide a robust parameter optimization framework for variational penalties in QSM reconstruction. The L-curve–based zero-curvature search produced almost optimal results for typical QSM acquisition settings. The frequency analysis method may use a 1.5 to 2.0 correction factor to

apply it as a stand-alone method for a wider range of signal-to-noise-ratio settings. This approach may also benefit from fast search algorithms such as the binary search to speed up the process.

Della Maggiora G., Castillo-Passi C., Qiu W., Liu S., Milovic C., Sekino M., Tejos C., Uribe S., Irarrazaval P. (2020)
DeepSPIO: Super Paramagnetic Iron Oxide Particle Quantification using Deep Learning in Magnetic Resonance Imaging.
Revista: IEEE Transactions on Pattern Analysis and Machine Intelligence, July 2020
Abstract: The susceptibility of Super Paramagnetic Iron Oxide (SPIO) particles makes them a useful contrast agent for different purposes in MRI. These particles are typically quantified with relaxometry or by measuring the inhomogeneities they produced. These methods rely on the phase, which is unreliable for high concentrations. We present in this study a novel Deep Learning method to quantify the SPIO concentration distribution. We acquired the data with a new sequence called View Line in which the field map information is encoded in the geometry of the image. The novelty of our network is that it uses residual blocks as the bottleneck and multiple decoders to improve the gradient flow in the network. Each decoder predicts a different part of the wavelet decomposition of the concentration map. This decomposition improves the estimation of the concentration, and also it accelerates the convergence of the model. We tested our SPIO concentration reconstruction technique with simulated images and data from actual scans from phantoms. The simulations were done using images from the IXI dataset, and the phantoms consisted of plastic cylinders containing agar with SPIO particles at different concentrations. In both experiments, the model was able to quantify the distribution accurately.

Arrieta C., Sing-Long C., Mura J., Irarrazaval P., Andia M., Uribe s., Tejos C. (2020)
Level set segmentation with shape prior knowledge using intrinsic rotation, translation and scaling alignment.
Revista: Biomedical Signal Processing and Control Volume 63, January 2021, 102241
Abstract: Level set segmentation has been successfully used in several image applications. However, they perform poorly when applied to severely corrupted images or when the object's boundaries are blurred or occluded. Poor performance can be improved by introducing shape prior knowledge into the segmentation process by considering additional shape information from training examples. This can be achieved by adding a regularization term that penalizes shapes that differ from those learned from a training database. This regularizer must be invariant under translation, rotation and scaling transformations. Previous works have proposed coupling the curve evolution to a registration problem through an optimization procedure. This approach is slow and its results depend on how this optimization is implemented. An alternative approach introduced an intrinsic alignment, which normalizes each shape to be compared on a common coordinate system, avoiding the registration process. Nevertheless, the proposed intrinsic alignment considered only scaling and translation but not rotation, which is critical in several image applications. In this paper we present a new method to incorporate shape prior knowledge based on the intrinsic alignment approach, but extending it for scaling, translation and rotation invariance. Our approach uses a regularization term based on the eigenvalues and eigenvectors of the covariance matrix of each training shape, and this eigendecomposition dependency leads to a new set of evolution equations. We tested our regularizer, combined with Chan–Vese, in 2D and 3D synthetic and medical images, demonstrating the effectiveness of using shape priors with intrinsic scaling, translation and rotation alignment in different segmentation problems.

Varela-Mattatall G., Castillo-Passi C., Koch A., Mura J., Stirnberg R., Uribe S., Tejos C., Stöcker T., Irarrázaval P. (2020)
MAPL1: q?space reconstruction using L1?regularized mean apparent propagator.
Revista: Magnetic Resonance in Medicine Volume84, Issue4 October 2020 Pp 2219-2230
Abstract: Purpose: To improve the quality of mean apparent propagator (MAP) reconstruction from a limited number of q-space samples.
Methods: We implement an urn:x-wiley:07403194:media:mrm28268:mrm28268-math-0003-regularised MAP (MAPL1) to consider higher order basis functions and to improve the fit without increasing the number of q-space samples. We compare MAPL1 with

the least-squares optimization subject to non-negativity (MAP), and the Laplacian-regularized MAP (MAPL). We use simulations of crossing fibers and compute the normalized mean squared error (NMSE) and the Pearson's correlation coefficient to evaluate the reconstruction quality in q-space. We also compare coefficient-based diffusion indices in the simulations and in in vivo data.
Results: Results indicate that MAPL1 improves NMSE in 1 to 3% when compared to MAP or MAPL in a high undersampling regime. Additionally, MAPL1 produces more reproducible and accurate results for all sampling rates when there are enough basis functions to meet the sparsity criterion for the regularizer. These improved reconstructions also produce better coefficient-based diffusion indices for in vivo data.
Conclusions: Adding an urn:x-wiley:07403194:media:mrm28268:mrm28268-math-0004 regularizer to MAP allows the use of more basis functions and a better fit without increasing the number of q-space samples. The impact of our research is that a complete diffusion spectrum can be reconstructed from an acquisition time very similar to a diffusion tensor imaging protocol.

Milovic C., Tejos C., Acosta-Cabronero J., Özbay P.S., Schwesser F., Marques J.P, Irarrázaval P., Bilgic B., Langkammer C. (2020)
The 2016 QSM Challenge: Lessons learned and considerations for a future challenge design.
Revista: Magnetic Resonance in Medicine Volume84, Issue3 September 2020 Pp 1624-1637
Abstract: Purpose: The 4th International Workshop on MRI Phase Contrast and QSM (2016, Graz, Austria) hosted the first QSM Challenge. A single-orientation gradient recalled echo acquisition was provided, along with COSMOS and the χ33 STI component as ground truths. The submitted solutions differed more than expected depending on the error metric used for optimization and were generally over-regularized. This raised (unanswered) questions about the ground truths and the metrics utilized.
Methods: We investigated the influence of background field remnants by applying additional filters. We also estimated the anisotropic contributions from the STI tensor to the apparent susceptibility to amend the χ33 ground truth and to investigate the impact on the reconstructions. Lastly, we used forward simulations from the COSMOS reconstruction to investigate the impact noise had on the metric scores.
Results: Reconstructions compared against the amended STI ground truth returned lower errors. We show that the background field remnants had a minor impact in the errors. In the absence of inconsistencies, all metrics converged to the same regularization weights, whereas structural similarity index metric was more insensitive to such inconsistencies.
Conclusion: There was a mismatch between the provided data and the ground truths due to the presence of unaccounted anisotropic susceptibility contributions and noise. Given the lack of reliable ground truths when using in vivo acquisitions, simulations are suggested for future QSM Challenges.

ALVARO LORCA

Simsek Y., Sahin H., Lorca A., Santika W.G., Urmee T., Escobar R. (2020)
Comparison of energy scenario alternatives for Chile: Towards low-carbon energy transition by 2030.
IEEE Energy Volume 206, 1 September 2020, 118021
Abstract: The objective of the paper is to generate an energy and environmental model using LEAP to forecast energy demand, supply, emissions for Chile by 2030 and create scenarios considering different policies motivated by current policy as well as national and international commitments from Chile. This paper contributes to literature by developing a long-term energy plan including all sectors for Chile, describing energy scenario alternatives and analyzing current policy, nationally determined contributions and sustainable development goals. Results indicate that scenarios with significant energy demand

reduction for all sectors showed considerable emission reduction by 2030. In all scenarios, demand sector showed major contribution to emissions when compared to transformation sector. Although emissions from transformation sector demonstrate significant reduction by 2030, decrease in demand side is not clearly noticed for some scenarios. Chile requires appropriate energy efficiency and renewable energy policies for demand sides of sectors especially transport, mining and other industries to reduce emissions at demand-side as having decarbonization for transformation side. Scenarios including more wind, PVsolar, CSPsolar and hydropower plants reached more than 80% renewable electricity generation by 2030. Thus, cleaner production portfolio which results in fewer emissions and more diversification in terms of energy generation can be established in Chile.

Verástegui F., Lorca A., Negrete-Pincetic M., Olivares D. (2020)
Firewood Heat Electrification Impacts in the Chilean Power System.
Revista: Volume 144, September 2020, 111702
Abstract: Chile presents an extended use of low-quality firewood for residential heating. This raises serious concerns, mainly related to health problems due to particulate emissions from firewood combustion. Several initiatives have been considered by the Chilean government to address this, including heat electrification goals. In addition, the Chilean power system is undergoing a decarbonization process. This paper analyzes the impacts of firewood heat electrification over the Chilean power system's decarbonization process until 2044, based on a capacity expansion planning model and an estimation of firewood heat demand, to account for major changes in load shape and spatial distribution. The results show that there is a large increase in the power system total cost (ranging from 5.6% to 19.4%), with flexibility requirements becoming larger in the south. Technologies that strongly depend on local resource availability, such as wind and concentrated solar power, present changes in their systemic value, altering the need for storage and flexibility. Also, aspects such as household insulation, electrification efficiency, and smart heating technologies would significantly impact the process in terms of cost reduction and optimal generation mix. The policy implications for the Chilean power system are presented, within the broader discussion of the overall firewood problem.

Bernal R., Olivares D., Negrete M., Lorca A. (2020)
Management of EV Charging Stations under Advance Reservations Schemes in Electricity Markets.
Revista: Sustainable Energy Grids & Networks Volume 24, December 2020, 100388
Abstract: As electric vehicles surpassed the 5.1 million-vehicle threshold in 2018, charging stations are becoming a growing necessity to allow electric vehicles charging while parked away from home. In addition, by harnessing the inherent flexibility of the charging process, charging stations can also provide services to the grid, such as frequency and voltage regulation. However, given that full-charge using state-of-the-art technology can take a minimum of nearly 30 min, drivers may face queues and uncertainty on the availability of charging sockets. To address this issue this work presents a model to determine the optimal management of charging stations using advance reservations. In the model, charging stations are assumed to participate in the energy and regulation markets, in addition to providing charging services to the vehicles. On the other hand, users are modeled using Satisficing decision model. The optimal management strategies are characterized by different charging tariffs and reservation fees, and their impact is analyzed in terms of the resulting charging profiles and welfare of electric vehicle users.

VLADIMIR MARIANOV

Eiselt H.A., Marianov V. (2020)
Stability of utility functions and apportionment rules in location models.
Revista: TOP 28, pages772–792(2020)
Abstract: This paper investigates how demand is apportioned to facilities by customers, given that they apply one of a number of utility functions according to which they satisfy their demand at the facilities. After delineating the basic decision-making process, a number of reasonable assumptions are formulated regarding the behavior of the utility functions after a scaling of their different parameters. The individual apportionment rules are examined so as to whether or not they satisfy these assumptions. The results are of importance for decision-makers that must use these utility functions when facing locational decisions.

MATÍAS NEGRETE

Verástegui F., Lorca A., Negrete-Pincetic M., Olivares D. (2020)
Firewood Heat Electrification Impacts in the Chilean Power System.
Revista: Energy Policy Volume 144, September 2020, 111702
Abstract: Chile presents an extended use of low-quality firewood for residential heating. This raises serious concerns, mainly related to health problems due to particulate emissions from firewood combustion. Several initiatives have been considered by the Chilean government to address this, including heat electrification goals. In addition, the Chilean power system is undergoing a decarbonization process. This paper analyzes the impacts of firewood heat electrification over the Chilean power system's decarbonization process until 2044, based on a capacity expansion planning model and an estimation of firewood heat demand, to account for major changes in load shape and spatial distribution. The results show that there is a large increase in the power system total cost (ranging from 5.6% to 19.4%), with flexibility requirements becoming larger in the south. Technologies that strongly depend on local resource availability, such as wind and concentrated solar power, present changes in their systemic value, altering the need for storage and flexibility. Also, aspects such as household insulation, electrification efficiency, and smart heating technologies would significantly impact the process in terms of cost reduction and optimal generation mix. The policy implications for the Chilean power system are presented, within the broader discussion of the overall firewood problem.

Bernal R., Olivares D., Negrete M., Lorca A. (2020)
Management of EV Charging Stations under Advance Reservations Schemes in Electricity Markets.
Revista: Sustainable Energy Grids & Networks Volume 24, December 2020, 100388
Abstract: As electric vehicles surpassed the 5.1 million-vehicle threshold in 2018, charging stations are becoming a growing necessity to allow electric vehicles charging while parked away from home. In addition, by harnessing the inherent flexibility of the charging process, charging stations can also provide services to the grid, such as frequency and voltage regulation. However, given that full-charge using state-of-the-art technology can take a minimum of nearly 30 min, drivers may face queues and uncertainty on the availability of charging sockets. To address this issue this work presents a model to determine the optimal management of charging stations using advance reservations. In the model, charging stations are assumed to participate in the energy and regulation markets, in addition to providing charging services to the vehicles. On the other

hand, users are modeled using Satisficing decision model. The optimal management strategies are characterized by different charging tariffs and reservation fees, and their impact is analyzed in terms of the resulting charging profiles and welfare of electric vehicle users.

FELIPE NÚÑEZ

Gómez J., Rodríguez J., García C., Tarisciotti L., Flores-Bahamonde F., Pereda J., Nuñez F., Cipriano A., Salas J.C. (2020)
An Overview of Microgrids Challenges in the Mining Industry.
Revista: IEEE Access, vol. 8, pp. 191378-191393
Abstract: The transition from fossil fuels to renewable energies as power sources in the heavy industries is one of the main climate change mitigation strategies. The carbon footprint in mining is related to its inherent extraction process, its high demand of electric power and water, and the use of diesel. However, considering its particular power requirements, the integration of microgrids throughout the whole control hierarchy of mining industry is an emergent topic. This paper provides an overview of the opportunities and challenges derived from the synergy between microgrids and the mining industry. Bidirectional and optimal power flow, as well as the integration of power quality have been identified as microgrid features that could potentially enhance mining processes. Recommendations pertaining to the technological transition and the improvement of energy issues in mining environments are also highlighted in this work.

Suarez A., Núñez F., Rodríguez-Fernandez M. (2020)
Circadian Phase Prediction from Non-Intrusive and Ambulatory Physiological Data.
Revista: IEEE Journal of Biomedical and Health Informatics, doi: 10.1109/JBHI.2020.3019789.
Abstract: Chronotherapy aims to treat patients according to their endogenous biological rhythms and requires, therefore, knowing their circadian phase. Circadian phase is partially determined by genetics and, under natural conditions, is normally entrained by environmental signals (zeitgebers), predominantly by light. Physiological data such as melatonin concentration and core body temperature (CBT) have been used to estimate circadian phase. However, due to their expensive and intrusive obtention, other physiological variables that also present circadian rhythmicity, such as heart rate variability, skin temperature, activity, and body position, have recently been proposed in several studies to estimate circadian phase. This study aims to predict circadian phase using minimally intrusive ambulatory physiological data modeled with machine learning techniques. Two approaches were considered; first, time-series were used to train artificial neural networks (ANNs) that predict CBT and melatonin dynamics and, second, a novel approach that uses scalar variables to build regression models that predict the time of the minimum CBT and the dim light melatonin onset (DLMO). ANNs require less than 48 hours of minimally intrusive data collection to predict circadian phase with an accuracy of less than one hour. On the other hand, regression models that use only three variables (body mass index, activity, and heart rate) are simpler and show higher accuracy with less than one minute of error, although they require longer times of data collection. This is a promising approach that should be validated in further studies considering a broader population and a wider range of conditions, including circadian misalignment.

Langarica S., Pizarro G., Poblete P., Rodríguez F., Pereda J., Núñez F. (2020)
Denoising and Voltage Estimation in Modular Multilevel Converters Using Deep Neural-Networks.
Revista: IEEE Access, vol. 8, pp. 207973-207981
Abstract: Modular Multilevel Converters (MMCs) have become one of the most popular

power converters for medium/high power applications, from transmission systems to motor drives. However, to operate properly, MMCs require a considerable number of sensors and communication of sensitive data to a central controller, all under relevant electromagnetic interference produced by the high frequency switching of power semiconductors. This work explores the use of neural networks (NNs) to support the operation of MMCs by: i) denoising measurements, such as stack currents, using a blind autoencoder NN; and ii) estimating the sub-module capacitor voltages, using an encoder-decoder NN. Experimental results obtained with data from a three-phase MMC show that NNs can effectively clean sensor measurements and estimate internal states of the converter accurately, even during transients, drastically reducing sensing and communication requirements.

Herrera T., Núñez F. (2020)
Design and Prototyping of a Thread Border Router Based on a Non Network-co-Processor Architecture.
Revista: IEEE Access, vol. 8, pp. 60613-60625
Abstract: The IPv6-native home-area-network-oriented Thread protocol stack is currently attracting attention from both academic and commercial consumer electronics communities. In a Thread mesh deployment, as with any 6LoWPAN-based solution, a key element is the border router, since integration to the world-wide web depends exclusively on its performance. The typical architecture of a Thread border router involves a low-capable Thread-enabled device that acts as a slave of a more powerful host device owning a second networking interface, in what is known as a network-co-processor (NCP) architecture. To provide an alternative, this work focuses on the design and prototyping of a Thread border router using a non-NCP architecture. The challenges faced in implementing a non-NCP border router are detailed and a benchmark against a state-of-the-art NCP border router is presented. Results show that the non-NCP border router reduces the out-of-mesh latency by a factor of two. Immaturity of the IEEE 802.15.4 subsystem in the Linux kernel was evident during design and further work in such area is likely to improve dramatically the results obtained.

Langarica S., Núñez F. (2020)
Neuroevolutive Control of Industrial Processes Through Mapping Elites.
Revista: IEEE Transactions on Industrial Informatics, doi: 10.1109/TII.2020.3019846.
Abstract: Classical model-based control techniques used in process control applications present a trade-off between performance and computational load, specially when using complex nonlinear methods. Learning-based techniques that allow the controller to learn policies from data represent an appealing alternative with potential to reduce the computational burden of real-time optimization. This work presents an efficient learning-based neural controller, optimized using evolutionary algorithms, designed specially for maintaining diversity of individuals. The search of solutions is conducted in the parameters space of a population of deep neural networks, which are efficiently encoded with a novel compression algorithm. Evaluation against strong baselines demonstrates that the proposed controller achieves better performance in most of the chosen evaluation metrics. Results suggest that learning-based controllers are a promising option for next generation process control in the context of industry 4.0.

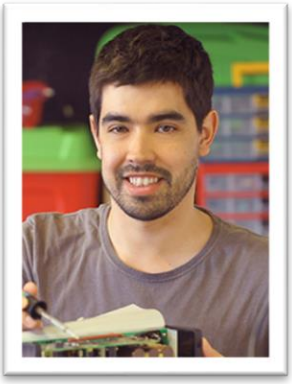

JAVIER PEREDA

Gómez J., Rodríguez J., García C., Tarisciotti L., Flores-Bahamonde F., Pereda J., Nuñez F., Cipriano A., Salas J.C. (2020)
An Overview of Microgrids Challenges in the Mining Industry.
Revista: IEEE Access, vol. 8, pp. 191378-191393
Abstract: The transition from fossil fuels to renewable energies as power sources in the heavy industries is one of the main climate

change mitigation strategies. The carbon footprint in mining is related to its inherent extraction process, its high demand of electric power and water, and the use of diesel. However, considering its particular power requirements, the integration of microgrids throughout the whole control hierarchy of mining industry is an emergent topic. This paper provides an overview of the opportunities and challenges derived from the synergy between microgrids and the mining industry. Bidirectional and optimal power flow, as well as the integration of power quality have been identified as microgrid features that could potentially enhance mining processes. Recommendations pertaining to the technological transition and the improvement of energy issues in mining environments are also highlighted in this work.

Langarica S., Pizarro G., Poblete P., Rodríguez F., Pereda J., Núñez F. (2020)
Denoising and Voltage Estimation in Modular Multilevel Converters Using Deep Neural-Networks.
Revista: IEEE Access, vol. 8, pp. 207973-207981
Abstract: Modular Multilevel Converters (MMCs) have become one of the most popular power converters for medium/high power applications, from transmission systems to motor drives. However, to operate properly, MMCs require a considerable number of sensors and communication of sensitive data to a central controller, all under relevant electromagnetic interference produced by the high frequency switching of power semiconductors. This work explores the use of neural networks (NNs) to support the operation of MMCs by: i) denoising measurements, such as stack currents, using a blind autoencoder NN; and ii) estimating the sub-module capacitor voltages, using an encoder-decoder NN. Experimental results obtained with data from a three-phase MMC show that NNs can effectively clean sensor measurements and estimate internal states of the converter accurately, even during transients, drastically reducing sensing and communication requirements.

Cuzmar R., Pereda J. Aguilera R.P. (2020)
Phase-Shifted Model Predictive Control to Achieve Power Balance of CHB Converters for Large-Scale Photovoltaic Integration.
Revista: IEEE Transactions on Industrial Electronics, doi: 10.1109/TIE.2020.3026299.
Abstract: Cascaded H-Bridge (CHB) converters are attractive candidates for next generation photovoltaic (PV) inverters. CHB converters present a reduced voltage stress per power switch and a high modularity. Therefore, the plant can be divided in several PV strings that can be connected to each H-bridge cell. However, due to variability on solar irradiance conditions, each PV string may present different maximum available power levels, which difficult the overall converter operation. To address this issue, this paper presents a model predictive control (MPC) strategy, which works along with a phase-shifted PWM (PS-PWM) stage; hence its name phase-shifted MPC (PS-MPC). The novelty of this proposal is the way both inter-bridge and inter-phase power imbalance are directly considered into the optimal control problem by a suitable system reference design. Thus, the inter-phase imbalance power is tackled by enforcing the converter to operate with a proper zero-sequence voltage component. Then, by exploiting the PS-PWM working principle, PS-MPC is able to handle each H-bridge cell independently. This allows the predictive controller to also deal with an inter-bridge power imbalance using the same control structure. Experimental results on a 3 kW prototype are provided to verify the effectiveness of the proposed PS-MPC strategy.

Azharuddin M., Rojas F., Cárdenas R., Pereda J., Díaz M., Kennel R. (2020)
Solid State Transformers: Concepts, Classification, and Control.
Revista: Energies 13(9), 2319
Abstract: Increase in global energy demand and constraints from fossil fuels have encouraged a growing share of renewable energy resources in the utility grid. Accordingly, an increased penetration of direct current (DC) power sources and loads (e.g., solar photovoltaics and electric vehicles) as well as the necessity for active power flow control has been witnessed in the power distribution networks. Passive transformers are susceptible to DC offset and possess no controllability when employed in smart grids. Solid state transformers (SSTs) are identified as a potential solution to modernize and harmonize alternating current (AC) and DC electrical networks and as suitable solutions in applications such as traction, electric ships, and aerospace industry. This paper provides a

complete overview on SST: concepts, topologies, classification, power converters, material selection, and key aspects for design criteria and control schemes proposed in the literature. It also proposes a simple terminology to identify and homogenize the large number of definitions and structures currently reported in the literature.

Neira S., Pereda J., Rojas F. (2020)
Three-Port Full-Bridge Bidirectional Converter for Hybrid DC/DC/AC Systems.
Revista: IEEE Transactions on Power Electronics, vol. 35, no. 12, pp. 13077-13084
Abstract: Sustainable solutions such as renewable energies, distributed generation, energy storage, and electric vehicles require power conversion and advance control techniques. This process is usually done in two stages by more than one power converter, specially in hybrid systems, increasing power losses and costs. The configuration with two dc stages and one ac port is widely used in several applications, such as grid-connected photovoltaic inverters; fuel cells, hybrid and electric vehicles; and ac/dc microgrids. Thus, three-port topologies have been developed to operate such systems, most of them comprising multiple power processing stages for the connection of the different elements. This article proposes a three-port full-bridge converter with a single power processing stage for dc/dc/ac systems. The ac port can be single-phase or three-phase, using two legs like an H-bridge or three legs like the conventional three-phase inverter. In both configurations, each leg is used as an inverter and as a buck-boost converter at the same time. The converter is able to manage the power flow among three ports with just four or six switches through a multivariable control strategy. Simulation and experimental results show the capability of the converter to manage the interaction between a battery and a capacitor connected to the grid achieving a fast dynamic response, bidirectional capability in all ports and reduction of components.

CLAUDIA PRIETO

Cruz G., Jaubert O., Qi H., Bustin A., Milotta G., Schneider T., Koken P., Doneva M., Botnar R.M., Prieto C. (2020)
3D free-breathing cardiac magnetic resonance fingerprinting.
Revista : NMR in Biomedicine 21 July 2020
Abstract: Purpose: To develop a novel respiratory motion compensated three-dimensional (3D) cardiac magnetic resonance fingerprinting (cMRF) approach for whole-heart myocardial T1 and T2 mapping from a free-breathing scan.
Methods: Two-dimensional (2D) cMRF has been recently proposed for simultaneous, co-registered T1 and T2 mapping from a breath-hold scan; however, coverage is limited. Here we propose a novel respiratory motion compensated 3D cMRF approach for whole-heart myocardial T1 and T2 tissue characterization from a free-breathing scan. Variable inversion recovery and T2 preparation modules are used for parametric encoding, respiratory bellows driven localized autofocus is proposed for beat-to-beat translation motion correction and a subspace regularized reconstruction is employed to accelerate the scan. The proposed 3D cMRF approach was evaluated in a standardized T1/T2 phantom in comparison with reference spin echo values and in 10 healthy subjects in comparison with standard 2D MOLLI, SASHA and T2-GraSE mapping techniques at 1.5 T.
Results: 3D cMRF T1 and T2 measurements were generally in good agreement with reference spin echo values in the phantom experiments, with relative errors of 2.9% and 3.8% for T1 and T2 (T2 < 100 ms), respectively. in vivo left ventricle (LV) myocardial T1 values were 1054 ± 19 ms for MOLLI, 1146 ± 20 ms for SASHA and 1093 ± 24 ms for the proposed 3D cMRF; corresponding T2 values were 51.8 ± 1.6

ms for T2-GraSE and 44.6 ± 2.0 ms for 3D cMRF. LV coefficients of variation were 7.6 ± 1.6% for MOLLI, 12.1 ± 2.7% for SASHA and 5.8 ± 0.8% for 3D cMRF T1, and 10.5 ± 1.4% for T2-GraSE and 11.7 ± 1.6% for 3D cMRF T2.
Conclusion: The proposed 3D cMRF can provide whole-heart, simultaneous and co-registered T1 and T2 maps with accuracy and precision comparable to those of clinical standards in a single free-breathing scan of about 7 min.

Milotta G, Bustin A, Jaubert O, Neji R, Prieto C, Botnar RM. (2020)
3D whole heart isotropic resolution motion compensated joint T1/T2 mapping and water/fat imaging.
Revista: Magnetic Resonance in Medicine Volume84, Issue6 December 2020 Pp 3009-3026
Abstract: Purpose: To develop a free-breathing isotropic-resolution whole-heart joint T1 and T2 mapping sequence with Dixon-encoding that provides coregistered 3D T1 and T2 maps and complementary 3D anatomical water and fat images in a single ~9 min scan.
Methods: Four interleaved dual-echo Dixon gradient echo volumes are acquired with a variable density Cartesian trajectory and different preparation pulses: 1) inversion recovery-preparation, 2) and 3) no preparations, and 4) T2 preparation. Image navigators are acquired to correct each echo for 2D translational respiratory motion; the 8 echoes are jointly reconstructed with a low-rank patch-based reconstruction. A water/fat separation algorithm is used to obtain water and fat images for each acquired volume. T1 and T2 maps are generated by matching the signal evolution of the water images to a simulated dictionary. Complementary bright-blood and fat volumes for anatomical visualization are obtained from the T2-prepared dataset. The proposed sequence was tested in phantom experiments and 10 healthy subjects and compared to standard 2D MOLLI T1 mapping, 2D balance steady-state free precession T2 mapping, and 3D T2-prepared Dixon coronary MR angiography.
Results: High linear correlation was found between T1 and T2 quantification with the proposed approach and phantom spin echo measurements (y = 1.1 × −11.68, R2 = 0.98; and y = 0.85 × +5.7, R2 = 0.99). Mean myocardial values of T1/T2 = 1116 ± 30.5 ms/45.1 ± 2.38 ms were measured in vivo. Biases of T1/T2 = 101.8 ms/−0.77 ms were obtained compared to standard 2D techniques.
Conclusion: The proposed joint T1/T2 sequence permitted the acquisition of motion-compensated isotropic-resolution 3D T1 and T2 maps and complementary coronary MR angiography and fat volumes, showing promising results in terms of T1 and T2 quantification and visualization of cardiac anatomy and pericardial fat.

Milotta G., Ginami G., Bustin A., Neji R., Prieto C., Botnar R.M. (2020)
3D whole-heart free-breathing qBOOST-T2 mapping.
Revista: Magnetic Resonance in Medicine Volume83, Issue5 May 2020 Pp 1673-1687
Abstract: Purpose: To develop an accelerated motion corrected 3D whole-heart imaging approach (qBOOST-T2) for simultaneous high-resolution bright- and black-blood cardiac MR imaging and quantitative myocardial T2 characterization.
Methods: Three undersampled interleaved balanced steady-state free precession cardiac MR volumes were acquired with a variable density Cartesian trajectory and different magnetization preparations: (1) T2-prepared inversion recovery (T2prep-IR), (2) T2-preparation, and (3) no preparation. Image navigators were acquired prior the acquisition to correct for 2D translational respiratory motion. Each 3D volume was reconstructed with a low-rank patch-based reconstruction. The T2prep-IR volume provides bright-blood anatomy visualization, the black-blood volume is obtained by means of phase sensitive reconstruction between first and third datasets, and T2 maps are generated by matching the signal evolution to a simulated dictionary. The proposed sequence has been evaluated in simulations, phantom experiments, 11 healthy subjects and compared with 3D bright-blood cardiac MR and standard 2D breath-hold balanced steady-state free precession T2 mapping. The feasibility of the proposed approach was tested on 4 patients with suspected cardiovascular disease.
Results: High linear correlation (y = 1.09 × −0.83, R2 = 0.99) was found between the proposed qBOOST-T2 and T2 spin echo measurements in phantom experiment. Good image quality was observed in vivo with the proposed 4x undersampled qBOOST-T2. Mean T2 values of 53.1 ± 2.1 ms and 55.8 ± 2.7 ms were measured

in vivo for 2D balanced steady-state free precession T2 mapping and qBOOST-T2, respectively, with linear correlation of y = 1.02x+1.46 (R2 = 0.61) and T2 bias = 2.7 ms.
Conclusion: The proposed qBOOST-T2 sequence allows the acquisition of 3D high-resolution co-registered bright- and black-blood volumes and T2 maps in a single scan of ~11 min, showing promising results in terms of T2 quantification.

Bustin A. , Rashid I, Cruz G, Hajhosseiny R., Correia T., Neji R., Rajani R., Ismail T., Botnar R.M., Prieto C. (2020)
3D Whole-Heart Isotropic Sub-Millimeter Resolution Coronary Magnetic Resonance Angiography with Non-Rigid Motion-Compensated PROST.
Revista : Journal of Cardiovascular Magnetic Resonance volume 22, Article number: 24 (2020)
Abstract: Background: To enable free-breathing whole-heart sub-millimeter resolution coronary magnetic resonance angiography (CMRA) in a clinically feasible scan time by combining low-rank patch-based undersampled reconstruction (3D-PROST) with a highly accelerated non-rigid motion correction framework.
Methods: Non-rigid motion corrected CMRA combined with 2D image-based navigators has been previously proposed to enable 100% respiratory scan efficiency in modestly undersampled acquisitions. Achieving sub-millimeter isotropic resolution with such techniques still requires prohibitively long acquisition times. We propose to combine 3D-PROST reconstruction with a highly accelerated non-rigid motion correction framework to achieve sub-millimeter resolution CMRA in less than 10 min. Ten healthy subjects and eight patients with suspected coronary artery disease underwent 4–5-fold accelerated free-breathing whole-heart CMRA with 0.9 mm3 isotropic resolution. Vessel sharpness, vessel length and image quality obtained with the proposed non-rigid (NR) PROST approach were compared against translational correction only (TC-PROST) and a previously proposed NR motion-compensated technique (non-rigid SENSE) in healthy subjects. For the patient study, image quality scoring and visual comparison with coronary computed tomography angiography (CCTA) were performed.
Results: Average scan times [min:s] were 6:01 ± 0:59 (healthy subjects) and 8:29 ± 1:41 (patients). In healthy subjects, vessel sharpness of the left anterior descending (LAD) and right (RCA) coronary arteries were improved with the proposed non-rigid PROST (LAD: 51.2 ± 8.8%, RCA: 61.2 ± 9.1%) in comparison to TC-PROST (LAD: 43.8 ± 5.1%, P = 0.051, RCA: 54.3 ± 8.3%, P = 0.218) and non-rigid SENSE (LAD: 46.1 ± 5.8%, P = 0.223, RCA: 56.7 ± 9.6%, P = 0.50), although differences were not statistically significant. The average visual image quality score was significantly higher for NR-PROST (LAD: 3.2 ± 0.6, RCA: 3.3 ± 0.7) compared with TC-PROST (LAD: 2.1 ± 0.6, P = 0.018, RCA: 2.0 ± 0.7, P = 0.014) and non-rigid SENSE (LAD: 2.3 ± 0.5, P = 0.008, RCA: 2.5 ± 0.7, P = 0.016). In patients, the proposed approach showed good delineation of the coronaries, in agreement with CCTA, with image quality scores and vessel sharpness similar to that of healthy subjects.
Conclusions: We demonstrate the feasibility of combining high undersampling factors with non-rigid motion-compensated reconstruction to obtain high-quality sub-millimeter isotropic CMRA images in ~ 8 min. Validation in a larger cohort of patients with coronary artery disease is now warranted.

Fuin N., Bustin A., Kustner T., Oksuz I., Clough J., King A., Schnabel J., Botnar R.M., Prieto C. (2020)
A multi-scale variational neural network for accelerating motion-compensated whole-heart 3D coronary MR angiography.
Revista: Magnetic Resonance Imaging Volume 70, July 2020, Pages 155-167
Abstract: Purpose: To enable fast reconstruction of undersampled motion-compensated whole-heart 3D coronary magnetic resonance angiography (CMRA) by learning a multi-scale variational neural network (MS-VNN) which allows the acquisition of high-quality 1.2 × 1.2 × 1.2 mm isotropic volumes in a short and predictable scan time.
Methods: Eighteen healthy subjects and one patient underwent free-breathing 3D CMRA acquisition with variable density spiral-like Cartesian sampling, combined with 2D image navigators for translational motion estimation/compensation. The proposed MS-VNN learns two sets of kernels and activation functions for the magnitude and phase images of the complex-valued data. For the magnitude, a multi-scale approach is applied to better capture the small calibre of the coronaries. Ten subjects were considered for training and validation. Prospectively undersampled motion-

compensated data with 5-fold and 9-fold accelerations, from the remaining 9 subjects, were used to evaluate the framework. The proposed approach was compared to Wavelet-based compressed-sensing (CS), conventional VNN, and to an additional fully-sampled (FS) scan.
Results: The average acquisition time (m:s) was 4:11 for 5-fold, 2:34 for 9-fold acceleration and 18:55 for fully-sampled. Reconstruction time with the proposed MS-VNN was ~14 s. The proposed MS-VNN achieves higher image quality than CS and VNN reconstructions, with quantitative right coronary artery sharpness (CS:43.0%, VNN:43.9%, MS-VNN:47.0%, FS:50.67%) and vessel length (CS:7.4 cm, VNN:7.7 cm, MS-VNN:8.8 cm, FS:9.1 cm) comparable to the FS scan.
Conclusion: The proposed MS-VNN enables 5-fold and 9-fold undersampled CMRA acquisitions with comparable image quality that the corresponding fully-sampled scan. The proposed framework achieves extremely fast reconstruction time and does not require tuning of regularization parameters, offering easy integration into clinical workflow.

Bustin A., Milotta G., Ismaail T., Neji R., Botnar R.M., Prieto C. (2020)
Accelerated free-breathing whole-heart 3D T2 mapping with high isotropic resolution.
Revista : Magnetic Resonance in Medicine Volume83, Issue3 March 2020 Pp 988-1002
Abstract: Purpose: To enable free-breathing whole-heart 3D T2 mapping with high isotropic resolution in a clinically feasible and predictable scan time. This 3D motion-corrected undersampled signal matched (MUST) T2 map is achieved by combining an undersampled motion-compensated T2-prepared Cartesian acquisition with a high-order patch-based reconstruction.
Methods: The 3D MUST-T2 mapping acquisition consists of an electrocardiogram-triggered, T2-prepared, balanced SSFP sequence with nonselective saturation pulses. Three undersampled T2-weighted volumes are acquired using a 3D Cartesian variable-density sampling with increasing T2 preparation times. A 2D image-based navigator is used to correct for respiratory motion of the heart and allow 100% scan efficiency. Multicontrast high-dimensionality undersampled patch-based reconstruction is used in concert with dictionary matching to generate 3D T2 maps. The proposed framework was evaluated in simulations, phantom experiments, and in vivo (10 healthy subjects, 2 patients) with 1.5-mm3 isotropic resolution. Three-dimensional MUST-T2 was compared against standard multi-echo spin-echo sequence (phantom) and conventional breath-held single-shot 2D SSFP T2 mapping (in vivo).
Results: Three-dimensional MUST-T2 showed high accuracy in phantom experiments ($R2 > 0.99$). The precision of T2 values was similar for 3D MUST-T2 and 2D balanced SSFP T2 mapping in vivo (5 ± 1 ms versus 4 ± 2 ms, $P = .52$). Slightly longer T2 values were observed with 3D MUST-T2 in comparison to 2D balanced SSFP T2 mapping (50.7 ± 2 ms versus 48.2 ± 1 ms, $P < .05$). Preliminary results in patients demonstrated T2 values in agreement with literature values.
Conclusion: The proposed approach enables free-breathing whole-heart 3D T2 mapping with high isotropic resolution in about 8 minutes, achieving accurate and precise T2 quantification of myocardial tissue in a clinically feasible scan time.

Küstner T., Fuin N., Hammernik K., Bustin A., Qi H., Hajhosseiny R., Masci P.G., Neji R., Rueckert D., Botnar R.M., Prieto C. (2020)
CINENet: deep learning-based 3D cardiac CINE MRI reconstruction with multi-coil complex-valued 4D spatio-temporal convolutions.
Revista: Scientific Reports 10, Article number: 13710 (2020)
Abstract: Cardiac CINE magnetic resonance imaging is the gold-standard for the assessment of cardiac function. Imaging accelerations have shown to enable 3D CINE with left ventricular (LV) coverage in a single breath-hold. However, 3D imaging remains limited to anisotropic resolution and long reconstruction times. Recently deep learning has shown promising results for computationally efficient reconstructions of highly accelerated 2D CINE imaging. In this work, we propose a novel 4D (3D + time) deep learning-based reconstruction network, termed 4D CINENet, for prospectively undersampled 3D Cartesian CINE imaging. CINENet is based on (3 + 1)D complex-valued spatio-temporal convolutions and multi-coil data processing. We trained and evaluated the proposed CINENet on in-house acquired 3D CINE data of 20 healthy subjects and 15 patients with suspected cardiovascular disease. The proposed CINENet network outperforms

iterative reconstructions in visual image quality and contrast (+ 67% improvement). We found good agreement in LV function (bias ± 95% confidence) in terms of end-systolic volume (0 ± 3.3 ml), end-diastolic volume (− 0.4 ± 2.0 ml) and ejection fraction (0.1 ± 3.2%) compared to clinical gold-standard 2D CINE, enabling single breath-hold isotropic 3D CINE in less than 10 s scan and ~ 5 s reconstruction time.

Hajhosseiny R., Bustin A., Munoz C., Rashid I., Cruz G., Manning W.J., Prieto., Botnar R.M. (2020)
CORONARY MAGNETIC RESONANCE ANGIOGRAPHY: TECHNICAL INNOVATIONS LEADING US TO THE PROMISED LAND?
Revista : Coronary artery disease remains the leading cause of cardiovascular morbidity and mortality. Invasive X-ray angiography and coronary computed tomography angiography are established gold standards for coronary luminography. However, they expose patients to invasive complications, ionizing radiation, and iodinated contrast agents. Among a number of imaging modalities, coronary cardiovascular magnetic resonance (CMR) angiography may be used in some cases as an alternative for the detection and monitoring of coronary arterial stenosis, with advantages including its versatility, excellent soft tissue characterization, and avoidance of ionizing radiation and iodinated contrast agents. In this review, we explore the recent advances in motion correction, image acceleration, and reconstruction technologies that are bringing coronary CMR angiography closer to widespread clinical implementation.

Nordio G., Bustin A., Odille F., Schneider T., Henningsson M., Prieto C., Botnar R.M. (2020)
Faster 3D saturation-recovery based myocardial T1 mapping using a reduced number of saturation points and denoising.
Revista: PLOS One April 10, 2020
Abstract: Purpose: To accelerate the acquisition of free-breathing 3D saturation-recovery-based (SASHA) myocardial T1 mapping by acquiring fewer saturation points in combination with a post-processing 3D denoising technique to maintain high accuracy and precision.
Methods: 3D SASHA T1 mapping acquires nine T1-weighted images along the saturation recovery curve, resulting in long acquisition times. In this work, we propose to accelerate conventional cardiac T1 mapping by reducing the number of saturation points. High T1 accuracy and low standard deviation (as a surrogate for precision) is maintained by applying a 3D denoising technique to the T1-weighted images prior to pixel-wise T1 fitting. The proposed approach was evaluated on a T1 phantom and 20 healthy subjects, by varying the number of T1-weighted images acquired between three and nine, both prospectively and retrospectively. Following the results from the healthy subjects, three patients with suspected cardiovascular disease were acquired using five T1-weighted images. T1 accuracy and precision was determined for all the acquisitions before and after denoising.
Results: In the T1 phantom, no statistical difference was found in terms of accuracy and precision for the different number of T1-weighted images before or after denoising ($P = 0.99$ and $P = 0.99$ for accuracy, $P = 0.64$ and $P = 0.42$ for precision, respectively). In vivo, both prospectively and retrospectively, the precision improved considerably with the number of T1-weighted images employed before denoising ($P<0.05$) but was independent on the number of T1-weighted images after denoising.
Conclusion: We demonstrate the feasibility of accelerating 3D SASHA T1 mapping by reducing the number of acquired T1-weighted images in combination with an efficient 3D denoising, without affecting accuracy and precision of T1 values.

Jaubert O., Cruz G., Bustin A., Schneider T., Koken P., Doneva M., Rueckert D., Botnar R.M., Prieto C. (2020)
Free-running cardiac magnetic resonance fingerprinting: Joint T1/T2 map and Cine imaging.
Revista: Magnetic Resonance Imaging Volume 68, May 2020, Pages 173-182
Abstract: Purpose: To develop and evaluate a novel non-ECG triggered 2D magnetic resonance fingerprinting (MRF) sequence allowing for simultaneous myocardial T1 and T2 mapping and cardiac Cine imaging.
Methods: Cardiac MRF (cMRF) has been recently proposed to provide joint T1/T2 myocardial mapping by triggering the acquisition to mid-diastole and relying on a subject-dependent dictionary of MR signal evolutions to generate the maps. In this work, we propose a novel “free-running” (non-ECG triggered) cMRF framework for simultaneous

myocardial T1 and T2 mapping and cardiac Cine imaging in a single scan. Free-running cMRF is based on a transient state bSSFP acquisition with tiny golden angle radial readouts, varying flip angle and multiple adiabatic inversion pulses. The acquired data is retrospectively gated into several cardiac phases, which are reconstructed with an approach that combines parallel imaging, low rank modelling and patch-based high-order tensor regularization. Free-running cMRF was evaluated in a standardized phantom and ten healthy subjects. Comparison with reference spin-echo, MOLLI, SASHA, T2-GRASE and Cine was performed.

Results: T1 and T2 values obtained with the proposed approach were in good agreement with reference phantom values (ICC(A,1) > 0.99). Reported values for myocardium septum T1 were 1043 ± 48 ms, 1150 ± 100 ms and 1160 ± 79 ms for MOLLI, SASHA and free-running cMRF respectively and for T2 of 51.7 ± 4.1 ms and 44.6 ± 4.1 ms for T2-GRASE and free-running cMRF respectively. Good agreement was observed between free-running cMRF and conventional Cine 2D ejection fraction (bias = −0.83%).

Conclusion: The proposed free-running cardiac MRF approach allows for simultaneous assessment of myocardial T1 and T2 and Cine imaging in a single scan.

Bustin A., Fuin N., Botnar R.M., Prieto C. (2020) From Compressed-Sensing to Artificial Intelligence-Based Cardiac MRI Reconstruction.

Revista: Frontiers in Cardiovascular Medicine 25 February 2020

Abstract: Cardiac magnetic resonance (CMR) imaging is an important tool for the non-invasive assessment of cardiovascular disease. However, CMR suffers from long acquisition times due to the need of obtaining images with high temporal and spatial resolution, different contrasts, and/or whole-heart coverage. In addition, both cardiac and respiratory-induced motion of the heart during the acquisition need to be accounted for, further increasing the scan time. Several undersampling reconstruction techniques have been proposed during the last decades to speed up CMR acquisition. These techniques rely on acquiring less data than needed and estimating the non-acquired data exploiting some sort of prior information. Parallel imaging and compressed sensing undersampling reconstruction techniques have revolutionized the field, enabling 2- to 3-fold scan time accelerations to become standard in clinical practice. Recent scientific advances in CMR reconstruction hinge on the thriving field of artificial intelligence. Machine learning reconstruction approaches have been recently proposed to learn the non-linear optimization process employed in CMR reconstruction. Unlike analytical methods for which the reconstruction problem is explicitly defined into the optimization process, machine learning techniques make use of large data sets to learn the key reconstruction parameters and priors. In particular, deep learning techniques promise to use deep neural networks (DNN) to learn the reconstruction process from existing datasets in advance, providing a fast and efficient reconstruction that can be applied to all newly acquired data. However, before machine learning and DNN can realize their full potentials and enter widespread clinical routine for CMR image reconstruction, there are several technical hurdles that need to be addressed. In this article, we provide an overview of the recent developments in the area of artificial intelligence for CMR image reconstruction. The underlying assumptions of established techniques such as compressed sensing and low-rank reconstruction are briefly summarized, while a greater focus is given to recent advances in dictionary learning and deep learning based CMR reconstruction. In particular, approaches that exploit neural networks as implicit or explicit priors are discussed for 2D dynamic cardiac imaging and 3D whole-heart CMR imaging. Current limitations, challenges, and potential future directions of these techniques are also discussed.

Küstner T, Bustin A, Jaubert O, Hajhosseiny R., Masci P.G., Neji R., Botnar R., Prieto C. (2020) Fully self-gated free-running 3D Cartesian cardiac CINE with isotropic whole-heart coverage in less than 2 min.

Revista: NMR in Biomedicine 25 September 2020

Abstract: Purpose: To develop a novel fast water-selective free-breathing 3D Cartesian cardiac CINE scan with full self-navigation and isotropic whole-heart (WH) coverage.

Methods: A free-breathing 3D Cartesian cardiac CINE scan with a water-selective balanced steady-state free precession and a continuous (non-ECG-gated) variable-density Cartesian

sampling with spiral profile ordering, out-inward sampling and acquisition-adaptive alternating tiny golden and golden angle increment between spiral arms is proposed. Data is retrospectively binned based on respiratory and cardiac self-navigation signals. A translational respiratory-motion-corrected and cardiac-motion-resolved image is reconstructed with a multi-bin patch-based low-rank reconstruction (MB-PROST) within about 15 min. A respiratory-motion-resolved approach is also investigated. The proposed 3D Cartesian cardiac CINE is acquired in sagittal orientation in 1 min 50 s for 1.9 mm3 isotropic WH coverage. Left ventricular (LV) function parameters and image quality derived from a blinded reading of the proposed 3D CINE framework are compared against conventional multi-slice 2D CINE imaging in 10 healthy subjects and 10 patients with suspected cardiovascular disease.
Results: The proposed framework provides free-breathing 3D cardiac CINE images with 1.9 mm3 spatial and about 45 ms temporal resolution in a short acquisition time (<2 min). LV function parameters derived from 3D CINE were in good agreement with 2D CINE (10 healthy subjects and 10 patients). Bias and confidence intervals were obtained for end-systolic volume, end-diastolic volume and ejection fraction of 0.1 ± 3.5 mL, −0.6 ± 8.2 mL and −0.1 ± 2.2%, respectively.
Conclusion: The proposed framework enables isotropic 3D Cartesian cardiac CINE under free breathing for fast assessment of cardiac anatomy and function.

Bustin A., Lima da Cruz G., Jaubert O., Lopez K., Botnar R.M., Prieto C. (2020)
High-dimensionality undersampled patch-based reconstruction (HD-PROST) for accelerated multi-contrast MRI.
Revista: Magnetic Resonance in Medicine Volume81, Issue6 June 2019 Pp 3705-3719
Abstract: Purpose: To develop a new high-dimensionality undersampled patch-based reconstruction (HD-PROST) for highly accelerated 2D and 3D multi-contrast MRI.
Methods: HD-PROST jointly reconstructs multi-contrast MR images by exploiting the highly redundant information, on a local and non-local scale, and the strong correlation shared between the multiple contrast images. This is achieved by enforcing multi-dimensional low-rank in the undersampled images. 2D magnetic resonance fingerprinting (MRF) phantom and in vivo brain acquisitions were performed to evaluate the performance of HD-PROST for highly accelerated simultaneous T1 and T2 mapping. Additional in vivo experiments for reconstructing multiple undersampled 3D magnetization transfer (MT)-weighted images were conducted to illustrate the impact of HD-PROST for high-resolution multi-contrast 3D imaging.
Results: In the 2D MRF phantom study, HD-PROST provided accurate and precise estimation of the T1 and T2 values in comparison to gold standard spin echo acquisitions. HD-PROST achieved good quality maps for the in vivo 2D MRF experiments in comparison to conventional low-rank inversion reconstruction. T1 and T2 values of white matter and gray matter were in good agreement with those reported in the literature for MRF acquisitions with reduced number of time point images (500 time point images, ~2.5 s scan time). For in vivo MT-weighted 3D acquisitions (6 different contrasts), HD-PROST achieved similar image quality than the fully sampled reference image for an undersampling factor of 6.5-fold.
Conclusion: HD-PROST enables multi-contrast 2D and 3D MR images in a short acquisition time without compromising image quality. Ultimately, this technique may increase the potential of conventional parameter mapping.

Küstner T., Bustin A., Jaubert O., Hajhosseiny R., Masci P.G., Neji R., Botnar R.M., Prieto C. (2020)
Isotropic 3D Cartesian single breath-hold CINE MRI with multi-bin patch-based low-rank reconstruction.
Revista: Magnetic Resonance in Medicine Volume84, Issue4 October 2020Pp. 218-2033
Abstract: Purpose: To develop a novel acquisition and reconstruction framework for isotropic 3D Cartesian cardiac CINE within a single breath-hold for left ventricle (LV) and whole-heart coverage.
Methods: A variable-density Cartesian acquisition with spiral profile ordering, out-inward sampling, and acquisition-adaptive alternating tiny golden/golden angle increment between spiral arms is proposed to provide incoherent and nonredundant sampling within and among cardiac phases. A novel multi-bin patch-based low-rank reconstruction, named MB-PROST, is proposed to exploit redundant information on a local (within a patch), nonlocal

(similar patches within a spatial neighborhood), and temporal (among all cardiac phases) scale with an implicit motion alignment among patches. The proposed multi-bin patch-based low-rank reconstruction reconstruction is compared against compressed sensing reconstruction, whereas LV function parameters derived from the proposed 3D CINE framework are compared against those estimated from conventional multislice 2D CINE imaging in 10 healthy subjects and 15 patients.
Results: The proposed framework provides 3D cardiac CINE images with high spatial (1.9 mm3) and temporal resolution (˜50 ms) in a single breath-hold of ˜20 s for LV and ˜26 s for whole-heart coverage in healthy subjects. Shorter breath-hold durations of ˜13 to 15 s are feasible for LV coverage with slightly anisotropic resolution (1.9 × 1.9 × 2.5 mm) in patients. LV function parameters derived from 3D CINE were in good agreement with 2D CINE, with a bias of −0.1 mL/0.1 mL, −0.9 mL/−1.0 mL, −0.1%/−0.8%; and confidence intervals of ±1.7 mL/±3.7 mL, ±1.2 mL/±2.6 mL, and ±1.2%/±3.6% (10 healthy subjects/15 patients) for end-systolic volume, end-diastolic volume, and ejection fraction, respectively.
Conclusion: The proposed framework enables 3D isotropic cardiac CINE in a single breath-hold scan of ˜20 s/˜26 s for LV/whole-heart coverage, showing good agreement with clinical 2D CINE scans in terms of LV functional assessment.

Munoz C., Cruz G., Neji R., Botnar R.M., Prieto C. (2020)
Motion corrected water/fat whole-heart coronary MR angiography with 100% respiratory efficiency.
Revista: Magnetic Resonance in Medicine Volume82, Issue2 August 2019 Pages 732-742
Abstract: Purpose: To develop a framework for respiratory motion-corrected 3D whole-heart water/fat coronary MR angiography (CMRA) at 3T with reduced and predictable scan time.
Methods: A 3D dual-echo acquisition and respiratory motion-corrected reconstruction framework for water/fat CMRA imaging was developed. The acquisition sequence integrates a 2D dual-echo image navigator (iNAV), enabling 100% respiratory scan efficiency. Respiratory motion estimated from both the 2D iNAVs and the 3D data itself is used to produce nonrigid motion-corrected water/fat CMRA images. A first study to investigate which iNAV (water, fat, in-phase or out-of-phase) provides the best translational motion estimation was performed in 10 healthy subjects. Subsequently, nonrigid motion-corrected water/fat images were compared to a diaphragmatic navigator gated and tracked water/fat CMRA acquisition. Image quality metrics included visible vessel length and vessel sharpness for both the left anterior descending and right coronary arteries.
Results: Average vessel sharpness achieved with water, fat, in-phase and out-of-phase iNAVs was 33.8%, 29.6%, 32.2%, and 38.5%, respectively. Out-of-phase iNAVs were therefore used for estimating translational respiratory motion for the remainder of the study. No statistically significant differences in vessel length and sharpness ($P > 0.01$) were observed between the proposed nonrigid motion correction approach and the reference images, although data acquisition was significantly shorter ($P < 2.6\times10–4$). Motion correction improved vessel sharpness by 60.4% and vessel length by 47.7%, on average, in water CMRA images in comparison with no motion correction.
Conclusion: The feasibility of a novel motion-corrected water/fat CMRA approach has been demonstrated at 3T, producing images comparable to a reference gated acquisition, but in a shorter and predictable scan time.

Jaubert O., Arrieta C., Cruz G., Bustin A., Schneider T., Georgiopoulos G., Masci P.G., Sing-Long C., Botnar R.M., Prieto C. (2020)
Multi-parametric Liver Tissue Characterization Using MR Fingerprinting: Simultaneous T1 , T2 , T2 *, and Fat Fraction Mapping.
Revista: Magnetic Resonance in Medicine 13 May 2020
Abstract: Purpose: Quantitative T1, T2, T2*, and fat fraction (FF) maps are promising imaging biomarkers for the assessment of liver disease, however these are usually acquired in sequential scans. Here we propose an extended MR fingerprinting (MRF) framework enabling simultaneous liver T1, T2, T2*, and FF mapping from a single ~14 s breath-hold scan.
Methods: A gradient echo (GRE) liver MRF sequence with nine readouts per TR, low flip angles (5-15°), varying magnetisation preparation and golden angle radial trajectory is acquired at 1.5T to encode T1, T2, T2*, and FF simultaneously. The nine-echo time-series are reconstructed using a low-rank tensor constrained reconstruction and used to fit T2*, B0 and to separate the water and fat signals.

Water- and fat-specific T1, T2, and M0 are obtained through dictionary matching, whereas FF estimation is extracted from the M0 maps. The framework was evaluated in a standardized T1/T2 phantom, a water-fat phantom, and 12 subjects in comparison to reference methods. Preliminary clinical feasibility is shown in four patients.
Results: The proposed water T1, water T2, T2*, and FF maps in phantoms showed high coefficients of determination ($r2 > 0.97$) relative to reference methods. Measured liver MRF values in vivo (mean ± SD) for T1, T2, T2*, and FF were 671 ± 60 ms, 43.2 ± 6.8 ms, 29 ± 6.6 ms, and 3.2 ± 2.6% with biases of 92 ms, −7.1 ms, −1.4 ms, and 0.63% when compared to conventional methods.
Conclusion: A nine-echo liver MRF sequence allows for quantitative multi-parametric liver tissue characterization in a single breath-hold scan of ~14 s. Future work will aim to validate the proposed approach in patients with liver disease.

Aizaz M., Moonen R.P.M., van der Pol J.A.J., Prieto C., Botnar R.M., Kooi M.E. (2020)
PET/MRI of atherosclerosis.
Revista: Cardiovascular Diagnosis & Therapy Vol 10, No 4 (August 2020)
Abstract: Myocardial infarction and stroke are the most prevalent global causes of death. Each year 15 million people worldwide die due to myocardial infarction or stroke. Rupture of a vulnerable atherosclerotic plaque is the main underlying cause of stroke and myocardial infarction. Key features of a vulnerable plaque are inflammation, a large lipid-rich necrotic core (LRNC) with a thin or ruptured overlying fibrous cap, and intraplaque hemorrhage (IPH). Noninvasive imaging of these features could have a role in risk stratification of myocardial infarction and stroke and can potentially be utilized for treatment guidance and monitoring. The recent development of hybrid PET/MRI combining the superior soft tissue contrast of MRI with the opportunity to visualize specific plaque features using various radioactive tracers, paves the way for comprehensive plaque imaging. In this review, the use of hybrid PET/MRI for atherosclerotic plaque imaging in carotid and coronary arteries is discussed. The pros and cons of different hybrid PET/MRI systems are reviewed. The challenges in the development of PET/MRI and potential solutions are described. An overview of PET and MRI acquisition techniques for imaging of atherosclerosis including motion correction is provided, followed by a summary of vessel wall imaging PET/MRI studies in patients with carotid and coronary artery disease. Finally, the future of imaging of atherosclerosis with PET/MRI is discussed.

Qi H., Bustin A., Kuestner T., Hajhosseiny R., Cruz G., Kunze K., Neji R., Botnar R.M., Prieto C. (2020)
Respiratory motion-compensated high-resolution 3D whole-heart T1r mapping.
Revista: Journal of Cardiovascular Magnetic Resonance 22, Article number: 12 (2020)
Abstract: Background:Cardiovascular magnetic resonance (CMR) T1ρ mapping can be used to detect ischemic or non-ischemic cardiomyopathy without the need of exogenous contrast agents. Current 2D myocardial T1ρ mapping requires multiple breath-holds and provides limited coverage. Respiratory gating by diaphragmatic navigation has recently been exploited to enable free-breathing 3D T1ρ mapping, which, however, has low acquisition efficiency and may result in unpredictable and long scan times. This study aims to develop a fast respiratory motion-compensated 3D whole-heart myocardial T1ρ mapping technique with high spatial resolution and predictable scan time.
Methods: The proposed electrocardiogram (ECG)-triggered T1ρ mapping sequence is performed under free-breathing using an undersampled variable-density 3D Cartesian sampling with spiral-like order. Preparation pulses with different T1ρ spin-lock times are employed to acquire multiple T1ρ-weighted images. A saturation prepulse is played at the start of each heartbeat to reset the magnetization before T1ρ preparation. Image navigators are employed to enable beat-to-beat 2D translational respiratory motion correction of the heart for each T1ρ-weighted dataset, after which, 3D translational registration is performed to align all T1ρ-weighted volumes. Undersampled reconstruction is performed using a multi-contrast 3D patch-based low-rank algorithm. The accuracy of the proposed technique was tested in phantoms and in vivo in 11 healthy subjects in comparison with 2D T1ρ mapping. The feasibility of the proposed technique was further investigated in 3 patients with suspected cardiovascular disease. Breath-hold late-gadolinium enhanced (LGE) images

were acquired in patients as reference for scar detection.
Results: Phantoms results revealed that the proposed technique provided accurate T1ρ values over a wide range of simulated heart rates in comparison to a 2D T1ρ mapping reference. Homogeneous 3D T1ρ maps were obtained for healthy subjects, with septal T1ρ of 58.0 ± 4.1 ms which was comparable to 2D breath-hold measurements (57.6 ± 4.7 ms, P = 0.83). Myocardial scar was detected in 1 of the 3 patients, and increased T1ρ values (87.4 ± 5.7 ms) were observed in the infarcted region.
Conclusions: An accelerated free-breathing 3D whole-heart T1ρ mapping technique was developed with high respiratory scan efficiency and near-isotropic spatial resolution (1.7 × 1.7 × 2 mm3) in a clinically feasible scan time of ~ 6 mins. Preliminary patient results suggest that the proposed technique may find applications in non-contrast myocardial tissue characterization.

Milotta G., Ginami G., Cruz G., Neji R., Prieto C., Botnar R.M. (2020)
Simultaneous 3D whole-heart bright-blood and black blood imaging for cardiovascular anatomy and wall assessment with interleaved T2 prep-IR.
Revista: Magnetic Resonance in Medicine Volume82, Issue1 July 2019 Pp 312-325
Abstract: Purpose: To develop a motion-corrected 3D flow-insensitive imaging approach interleaved T2 prepared-inversion recovery (iT2prep-IR) for simultaneous lumen and wall visualization of the great thoracic vessels and cardiac structures.
Methods: A 3D flow-insensitive approach for simultaneous cardiovascular lumen and wall visualization (iT2prep) has been previously proposed. This approach requires subject-dependent weighted subtraction to completely null the arterial blood signal in the black-blood volume. Here, we propose an (T2prep-IR) approach to improve wall visualization and remove need for weighted subtraction. The proposed sequence is based on the acquisition and direct subtraction of 2 interleaved 3D whole-heart data sets acquired with and without T2prep-IR preparation. Image navigators are acquired before data acquisition to enable 2D translational and 3D non-rigid motion correction allowing 100% respiratory scan efficiency. The proposed approach was evaluated in 10 healthy subjects and compared with the conventional 2D double inversion recovery (DIR) sequence and the 3D iT2prep sequence. Additionally, 5 patients with congenital heart disease were acquired to test the clinical feasibility of the proposed approach.
Results: The proposed iT2prep-IR sequence showed improved blood nulling compared to both DIR and iT2prep techniques in terms of SNR (SNRblood = 6.9, 12.2, and 18.2, respectively) and contrast-to-noise-ratio (CNRmyoc-blood = 28.4, 15.4, and 15.3, respectively). No statistical difference was observed between iT2prep-IR, iT2prep and DIR atrial and ventricular wall thickness quantification.
Conclusion: The proposed interleaved T2prep-IR sequence enables the simultaneous lumen and wall visualization of cardiac structures and shows promising results in terms of SNR, CNR, and wall thickness measurement.

Jaubert O., Cruz G., Bustin A., Lavin B., Koken P., Hajhosseiny R., Doneva M., Rueckert D., Botnar R.M., Prieto C. (2020)
Water/fat Dixon Cardiac Magnetic Resonance Fingerprinting.
Revista: Magnetic Resonance in Medicine Volume83, Issue 6 June 2020 Pp 2107-2123
Abstract: Purpose: Cardiac magnetic resonance fingerprinting (cMRF) has been recently introduced to simultaneously provide T1, T2, and M0 maps. Here, we develop a 3-point Dixon-cMRF approach to enable simultaneous water specific T1, T2, and M0 mapping of the heart and fat fraction (FF) estimation in a single breath-hold scan.
Methods: Dixon-cMRF is achieved by combining cMRF with several innovations that were previously introduced for other applications, including a 3-echo GRE acquisition with golden angle radial readout and a high-dimensional low-rank tensor constrained reconstruction to recover the highly undersampled time series images for each echo. Water–fat separation of the Dixon-cMRF time series is performed to allow for water- and fat-specific T1, T2, and M0 estimation, whereas FF estimation is extracted from the M0 maps. Dixon-cMRF was evaluated in a standardized T1–T2 phantom, in a water–fat phantom, and in healthy subjects in comparison to current clinical standards: MOLLI, SASHA, T2-GRASE, and 6-point Dixon proton density FF (PDFF) mapping.
Results: Dixon-cMRF water T1 and T2 maps showed good agreement with reference T1 and

T2 mapping techniques (R2 > 0.99 and maximum normalized RMSE ~5%) in a standardized phantom. Good agreement was also observed between Dixon-cMRF FF and reference PDFF (R2 > 0.99) and between Dixon-cMRF water T1 and T2 and water selective T1 and T2 maps (R2 > 0.99) in a water–fat phantom. In vivo Dixon-cMRF water T1 values were in good agreement with MOLLI and water T2 values were slightly underestimated when compared to T2-GRASE. Average myocardium septal T1 values were 1129 ± 38 ms, 1026 ± 28 ms, and 1045 ± 32 ms for SASHA, MOLLI, and the proposed water Dixon-cMRF. Average T2 values were 51.7 ± 2.2 ms and 42.8 ± 2.6 ms for T2-GRASE and water Dixon-cMRF, respectively. Dixon-cMRF FF maps showed good agreement with in vivo PDFF measurements (R2 > 0.98) and average FF in the septum was measured at 1.3%.
Conclusion: The proposed Dixon-cMRF allows to simultaneously quantify myocardial water T1, water T2, and FF in a single breath-hold scan, enabling multi-parametric T1, T2, and fat characterization. Moreover, reduced T1 and T2 quantification bias caused by water–fat partial volume was demonstrated in phantom experiments.

Nordio G., Schneider T., Cruz G., Correia T., Bustin A., Prieto C., Botnar R.M. (2020)
Whole-heart T1 mapping using a 2D fat image navigator for respiratory motion compensation.
Revista: Magnetic Resonance in Medicine Volume83, Issue 1 January 2020 Pp 178-187
Abstract: Purpose: To combine a 3D saturation-recovery-based myocardial T1 mapping (3D SASHA) sequence with a 2D image navigator with fat excitation (fat-iNAV) to allow 3D T1 maps with 100% respiratory scan efficiency and predictable scan time.
Methods: Data from T1 phantom and 10 subjects were acquired at 1.5T. For respiratory motion compensation, a 2D fat-iNAV was acquired before each 3D SASHA k-space segment to correct for 2D translational motion in a beat-to-beat fashion. The effect of the fat-iNAV on the 3D SASHA T1 estimation was evaluated on the T1 phantom. For 3 representative subjects, the proposed free-breathing 3D SASHA with fat-iNAV was compared to the original implementation with the diaphragmatic navigator. The 3D SASHA with fat-iNAV was compared to the breath-hold 2D SASHA sequence in terms of accuracy and precision.
Results: In the phantom study, the Bland-Altman plot shows that the 2D fat-iNAVs does not affect the T1 quantification of the 3D SASHA acquisition (0 ± 12.5 ms). For the in vivo study, the 2D fat-iNAV permits to estimate the respiratory motion of the heart, while allowing for 100% scan efficiency, improving the precision of the T1 measurement compared to non-motion-corrected 3D SASHA. However, the image quality achieved with the proposed 3D SASHA with fat-iNAV is lower compared to the original implementation, with reduced delineation of the myocardial borders and papillary muscles.
Conclusions: We demonstrate the feasibility to combine the 3D SASHA T1 mapping imaging sequence with a 2D fat-iNAV for respiratory motion compensation, allowing 100% respiratory scan efficiency and predictable scan time.

CRISTIAN TEJOS

Milovic C., Prieto C., Bilgic B., Uribe S., Acosta-Cabronero J., Irarrazaval P., Tejos C. (2020)
Comparison of parameter optimization methods for quantitative susceptibility mapping.
Revista: Magnetic Resonance in Medicine Volume85, Issue1 January 2021 Pp 480-494
Abstract: Purpose: Quantitative Susceptibility Mapping (QSM) is usually performed by minimizing a functional with data fidelity and regularization terms. A weighting parameter controls the balance between these terms. There is a need for techniques to find the proper balance that avoids artifact propagation and loss of details. Finding the point of maximum curvature in the L-curve is a popular choice,

although it is slow, often unreliable when using variational penalties, and has a tendency to yield overregularized results.
Methods: We propose 2 alternative approaches to control the balance between the data fidelity and regularization terms: 1) searching for an inflection point in the log-log domain of the L-curve, and 2) comparing frequency components of QSM reconstructions. We compare these methods against the conventional L-curve and U-curve approaches.
Results: Our methods achieve predicted parameters that are better correlated with RMS error, high-frequency error norm, and structural similarity metric-based parameter optimizations than those obtained with traditional methods. The inflection point yields less overregularization and lower errors than traditional alternatives. The frequency analysis yields more visually appealing results, although with larger RMS error.
Conclusion: Our methods provide a robust parameter optimization framework for variational penalties in QSM reconstruction. The L-curve–based zero-curvature search produced almost optimal results for typical QSM acquisition settings. The frequency analysis method may use a 1.5 to 2.0 correction factor to apply it as a stand-alone method for a wider range of signal-to-noise-ratio settings. This approach may also benefit from fast search algorithms such as the binary search to speed up the process.

della Maggiora G., Castillo-Passi C., Qiu W., Liu S., Milovic C., Sekino M., Tejos C., Uribe S., Irarrazaval P. (2020)
DeepSPIO: Super Paramagnetic Iron Oxide Particle Quantification using Deep Learning in Magnetic Resonance Imaging.
Revista : IEEE Transactions on Pattern Analysis and Machine Intelligence, doi: 10.1109/TPAMI.2020.3012103.
Abstract: The susceptibility of Super Paramagnetic Iron Oxide (SPIO) particles makes them a useful contrast agent for different purposes in MRI. These particles are typically quantified with relaxometry or by measuring the inhomogeneities they produced. These methods rely on the phase, which is unreliable for high concentrations. We present in this study a novel Deep Learning method to quantify the SPIO concentration distribution. We acquired the data with a new sequence called View Line in which the field map information is encoded in the geometry of the image. The novelty of our network is that it uses residual blocks as the bottleneck and multiple decoders to improve the gradient flow in the network. Each decoder predicts a different part of the wavelet decomposition of the concentration map. This decomposition improves the estimation of the concentration, and also it accelerates the convergence of the model. We tested our SPIO concentration reconstruction technique with simulated images and data from actual scans from phantoms. The simulations were done using images from the IXI dataset, and the phantoms consisted of plastic cylinders containing agar with SPIO particles at different concentrations. In both experiments, the model was able to quantify the distribution accurately.

Arrieta C., Sing-Long C., Mura J., Irarrazaval P., Andia M., Uribe s., Tejos C. (2020)
Level set segmentation with shape prior knowledge using intrinsic rotation, translation and scaling alignment.
Revista : Volume 63, January, 102241
Abstract: Level set segmentation has been successfully used in several image applications. However, they perform poorly when applied to severely corrupted images or when the object' s boundaries are blurred or occluded. Poor performance can be improved by introducing shape prior knowledge into the segmentation process by considering additional shape information from training examples. This can be achieved by adding a regularization term that penalizes shapes that differ from those learned from a training database. This regularizer must be invariant under translation, rotation and scaling transformations. Previous works have proposed coupling the curve evolution to a registration problem through an optimization procedure. This approach is slow and its results depend on how this optimization is implemented. An alternative approach introduced an intrinsic alignment, which normalizes each shape to be compared on a common coordinate system, avoiding the registration process. Nevertheless, the proposed intrinsic alignment considered only scaling and translation but not rotation, which is critical in several image applications. In this paper we present a new method to incorporate shape prior knowledge based on the intrinsic alignment approach, but extending it for scaling, translation and rotation invariance. Our approach uses a regularization term based on

the eigenvalues and eigenvectors of the covariance matrix of each training shape, and this eigendecomposition dependency leads to a new set of evolution equations. We tested our regularizer, combined with Chan–Vese, in 2D and 3D synthetic and medical images, demonstrating the effectiveness of using shape priors with intrinsic scaling, translation and rotation alignment in different segmentation problems.

Varela-Mattatall G., Castillo-Passi C., Koch A., Mura J., Stirnberg R., Uribe S., Tejos C., Stöcker T., Irarrázaval P. (2020)
MAPL1: q? space reconstruction using L1?regularized mean apparent propagator.
Revista : Magnetic Resonance in Medicine Volume84, Issue4 October 2020 Pp 2219-2230
Abstract: Purpose: To improve the quality of mean apparent propagator (MAP) reconstruction from a limited number of q-space samples.
Methods: We implement an urn:x-wiley:07403194:media:mrm28268:mrm28268-math-0003-regularised MAP (MAPL1) to consider higher order basis functions and to improve the fit without increasing the number of q-space samples. We compare MAPL1 with the least-squares optimization subject to non-negativity (MAP), and the Laplacian-regularized MAP (MAPL). We use simulations of crossing fibers and compute the normalized mean squared error (NMSE) and the Pearson's correlation coefficient to evaluate the reconstruction quality in q-space. We also compare coefficient-based diffusion indices in the simulations and in in vivo data.
Results: Results indicate that MAPL1 improves NMSE in 1 to 3% when compared to MAP or MAPL in a high undersampling regime. Additionally, MAPL1 produces more reproducible and accurate results for all sampling rates when there are enough basis functions to meet the sparsity criterion for the regularizer. These improved reconstructions also produce better coefficient-based diffusion indices for in vivo data.
Conclusions: Adding an urn:x-wiley:07403194:media:mrm28268:mrm28268-math-0004 regularizer to MAP allows the use of more basis functions and a better fit without increasing the number of q-space samples. The impact of our research is that a complete diffusion spectrum can be reconstructed from an acquisition time very similar to a diffusion tensor imaging protocol.

Milovic C., Tejos C., Acosta-Cabronero J., Özbay P.S., Schwesser F., Marques J.P, Irarrázaval P., Bilgic B., Langkammer C. (2020)
The 2016 QSM Challenge: Lessons learned and considerations for a future challenge design.
Revista : Magnetic Resonance in Medicine Volume84, Issue3 September 2020 Pp 1624-1637
Abstract: Purpose: The 4th International Workshop on MRI Phase Contrast and QSM (2016, Graz, Austria) hosted the first QSM Challenge. A single-orientation gradient recalled echo acquisition was provided, along with COSMOS and the χ33 STI component as ground truths. The submitted solutions differed more than expected depending on the error metric used for optimization and were generally over-regularized. This raised (unanswered) questions about the ground truths and the metrics utilized.
Methods: We investigated the influence of background field remnants by applying additional filters. We also estimated the anisotropic contributions from the STI tensor to the apparent susceptibility to amend the χ33 ground truth and to investigate the impact on the reconstructions. Lastly, we used forward simulations from the COSMOS reconstruction to investigate the impact noise had on the metric scores.
Results: Reconstructions compared against the amended STI ground truth returned lower errors. We show that the background field remnants had a minor impact in the errors. In the absence of inconsistencies, all metrics converged to the same regularization weights, whereas structural similarity index metric was more insensitive to such inconsistencies.
Conclusion: There was a mismatch between the provided data and the ground truths due to the presence of unaccounted anisotropic susceptibility contributions and noise. Given the lack of reliable ground truths when using in vivo acquisitions, simulations are suggested for future QSM Challenges.

MIGUEL TORRES

Rigotti-Thompson M., Torres-Torriti M., Cheein A., Troni G. (2020)
Hinf-based Terrain Disturbance Rejection for Hydraulically Actuated Mobile Manipulators with a Non-Rigid Link.
Revista: EEE/ASME Transactions on Mechatronics, vol. 25, no. 5, pp. 2523-2533, Oct. 2020.
Abstract: Decoupling the end-effector motion from that of the mobile base of mobile manipulators traversing uneven terrains is important. This is especially so in mining, where material spillage from excavators and front-end loaders reduces productivity and slows down operations because of increased clean-up and maintenance times. Thus, this article proposes a strategy that relies on H ∞ feedback control combined with feedforward action to improve the rejection of terrain disturbances that affect the orientation of the end-effector. The dynamic model of the mobile manipulator considers a floating base with nonpermanent contacts at each wheel, hydraulic actuators with nonlinear dynamics and a nonrigid arm. The arm flexibility is modeled as a passive spring-damper joint to account for inherent cantilever effects of real excavators and loaders. The analysis considers three different H ∞ controller structures (single-input single-output (SISO) with feedforward, single-input multiple-output without feedforward, and multiple-input multiple-output without feedforward) to determine the benefits or disadvantages of employing the pitch rate of the mobile base as a feedforward control action or as an input handled by the H ∞ controller and using only the end-effector actuator or also the other actuated joints of the arm. The root-mean-square error (RMSE) was reduced between 73.8%-86.0% when driving an industrial semiautonomous skid-steer loader over a ramp using the SISO H ∞ controller with feedforward action.The tilt angle error was kept on average less than 0.9 ± 0.1°. The same controller yields a reduction of the RMSE between 23.5%- 38.4% and a tilt angle error smaller than 3.39 ± 0.07° on average when traversing over a bump. Hence, the strategy proposed to reject ground disturbances should contribute to reducing material spillage of existing autonomous machines that navigate with little operator intervention along mining galleries, but that cannot avoid disturbing material lying.

Guevara J., Arevalo-Ramirez T., Yandun F., Torres-Torriti M., Cheein F.A. (2020)
Point cloud-based estimation of effective payload volume for earthmoving loaders.
Revista: Automation in Construction Volume 117, September 2020, 103207
Abstract: Construction and mining require high levels of planning and productivity. Planning and management of operational targets and performance requires taking into account several variables, among which the amount of moved, loaded and unloaded material is one the main ones. This motivates the development of an approach for the estimation of the volume of material transported in field operations by loader trucks. The proposed methodology employs a three-dimensional point cloud representation of the volume and is tested using a skid-steer loader. The volume estimation process involves the segmentation of the loader's bucket from the raw point cloud using machine learning techniques. The segmented point cloud is associated with a pre-constructed reference model of the empty bucket. The volume is computed from a surface model built using the alpha shape algorithm applied to the Delaunay triangulation of the segmented point cloud. Several field experiments were carried out using a stereo camera for five different volumes of material and the bucket at different heights. A 95% accuracy was obtained on average. The encouraging results suggest that effective volume estimation for different bucket types would be possible using the proposed methodology.

Pradi A.J., Torres-Torriti M., Yuz J., Cheein F.A. (2020)
Tube-based nonlinear model predictive control for autonomous skid-steer mobile robots with tire–terrain interactions.

Revista: Control Engineering Practice Volume 101, August 2020, 104451

Abstract: This work addresses the problem of robust tracking control for skid-steer mobile platforms, using tube-based Nonlinear Model Predictive Control. The strategy seeks to mitigate the impact of disturbances propagated to autonomous vehicles originated by traction losses. To this end, a dynamical model composed by two coupled sub-systems stands for lateral and longitudinal vehicle dynamics and tire behavior. The controller is aimed at tracking prescribed stable operation points of the slip and side-slip beyond the robot pose and speeds. To reach robust tracking performance on the global system, a centralized control scheme operates under a predictive control framework composed by three control actions. The first one compensates for disturbances using the reference trajectory-feedforward control. The second control action corrects the errors generated by the modeling mismatch. The third one is devoted to ensure robustness on the closed-loop system whilst compensating for deviations of the state trajectories from the nominal ones (i.e. disturbance-free). The strategy ensures robust feasibility even when tightening constraints are met. Such constraints are calculated on-line based on robust positively invariant sets characterized by polytopic sets (tubes), including a terminal region to guarantee robustness. The benefits of the controller regarding tracking performance, constraint satisfaction and computational practicability were tested through simulations with a Cat® 262C skid-steer model. Then, in field tests, the controller evidenced high tracking accuracy against terrain disturbances when benchmarking performance with respect to inherent robust predictive controllers.

LEONARDO VANZI

Dorval P., Talens G.J.J., Otten G.P.P., Brahm R., Jordán A., Torres P., Vanzi L., Zapata A., Henry T., Paredes L., Jao W.C., James H., Hinojosa R., Bakos G.A., Csubry Z., Bhatti W., Suc V., Osip D., Mamajek E.E., Mellon S.N., Wyttenbach A., Stuik R., Ke (2020)

MASCARA-4 b/bRing-1 b: A retrograde hot Jupiter around a bright A-type star.

Revista: Astronomy & Astrophysics Volume 635 (March 2020)

Abstract: Context. The Multi-site All-Sky CAmeRA (MASCARA) and bRing are both photometric ground-based instruments with multiple stations that rely on interline charge-coupled devices with wide-field lenses to monitor bright stars in the local sky for variability. MASCARA has already discovered several planets in the northern sky, which are among the brightest known transiting hot Jupiter systems. Aims. In this paper, we aim to characterize a transiting planetary candidate in the southern skies found in the combined MASCARA and bRing data sets of HD 85628, an A7V star of V = 8.2 mag at a distance 172 pc, to establish its planetary nature.

Methods. The candidate was originally detected in data obtained jointly with the MASCARA and bRing instruments using a Box Least-Square search for transit events. Further photometry was taken by the 0.7 m Chilean-Hungarian Automated Telescope (CHAT), and radial velocity measurements with the Fiber Dual Echelle Optical Spectrograph on the European Southern Observatory 1.0 m Telescope. High-resolution spectra during a transit were taken with the CTIO high-resolution spectrometer (CHIRON) on the Small and Moderate Aperture Research Telescope System 1.5 m telescope to target the Doppler shadow of the candidate.

Results. We confirm the existence of a hot Jupiter transiting the bright A7V star HD 85628, which we co-designate as MASCARA-4b and

bRing-1b. It is in an orbit of 2.824 days, with an estimated planet radius of 1.53−0.04+0.07 RJup and an estimated planet mass of 3.1 ± 0.9 MJup, putting it well within the planetary regime. The CHAT observations show a partial transit, reducing the probability that the transit was around a faint background star. The CHIRON observations show a clear Doppler shadow, implying that the transiting object is in a retrograde orbit with |λ| =244.9−3.6+2.7°. The planet orbits at a distance of 0.047 ± 0.004 AU from the star and has a zero-albedo equilibrium temperature of 2100 ± 100 K. In addition, we find that HD 85628 has a previously unreported stellar companion star in the Gaia DR2 data demonstrating common proper motion and parallax at 4.3'' separation (projected separation ~740 AU), and with absolute magnitude consistent with being a K/M dwarf.
Conclusions. MASCARA-4 b/bRing-1 b is the brightest transiting hot Jupiter known to date in a retrograde orbit. It further confirms that planets in near-polar and retrograde orbits are more common around early-type stars. Due to its high apparent brightness and short orbital period, the system is particularly well suited for further atmospheric characterization.

Brahm R., Nielsen L., Wittenmyer R.A., Wang S., Rodriguez J.E., Espinoza N., Jones M., Jordán A., Henning T., Hobson M., Kossakowski D., Rojas F., Sarkis P., Schlecker M., Trifonov T., Shahaf S., Ricker G., Vanderspek R., Latham D., Seager S., Winn J., (2020)
TOI-481 b and TOI-892 b: Two Long-period Hot Jupiters from the Transiting Exoplanet Survey Satellite.
Revista: Astronomical Journal Volume 160, Number 5
Abstract: We present the discovery of two new 10 day period giant planets from the Transiting Exoplanet Survey Satellite mission, whose masses were precisely determined using a wide diversity of ground-based facilities. TOI-481 b and TOI-892 b have similar radii (0.99 ± 0.01 ${R}_{{\rm{J}}}$ and 1.07 ± 0.02 ${R}_{{\rm{J}}}$, respectively), and orbital periods (10.3311 days and 10.6266 days, respectively), but significantly different masses (1.53 ± 0.03 ${M}_{{\rm{J}}}$ versus 0.95 ± 0.07 ${M}_{{\rm{J}}}$, respectively). Both planets orbit metal-rich stars ($[\mathrm{Fe}/{\rm{H}}]$ = $+0.26\pm 0.05$ dex and $[\mathrm{Fe}/{\rm{H}}]$ = $+0.24\pm 0.05$ for TOI-481 and TOI-892, respectively) but at different evolutionary stages. TOI-481 is a ${M}_{\star }$ = 1.14 ± 0.02 ${M}_{\odot }$, ${R}_{\star }$ = 1.66 ± 0.02 ${R}_{\odot }$ G-type star (${T}_{\mathrm{eff}}$ = 5735 ± 72 K), that with an age of 6.7 Gyr, is in the turn-off point of the main sequence. TOI-892 on the other hand, is a F-type dwarf star (${T}_{\mathrm{eff}}$ = 6261 ± 80 K), which has a mass of ${M}_{\star }$ = 1.28 ± 0.03 ${M}_{\odot }$ and a radius of ${R}_{\star }$ = 1.39 ± 0.02 ${R}_{\odot }$. TOI-481 b and TOI-892 b join the scarcely populated region of transiting gas giants with orbital periods longer than 10 days, which is important to constrain theories of the formation and structure of hot Jupiters.

IV. TITULADOS DE INGENIERIA ELECTRICA

TITULADOS DE INGENIERIA ELECTRICA

Ingeniero Civil Electricista	Ingeniero Civil de Industrias, Mención Ingeniería Eléctrica
CUZMAR, RODRIGO HERNÁN *	CHÁVEZ, NICOLÁS MATÍAS
CORTÉS, JULIO ESTEBAN	GREZ, HORACIO JOSÉ
CISTERNAS, GABRIEL ANDRÉS	GUTIÉRREZ, NICOLÁS ENRIQUE
CHAPARRO, FELIPE *	JACOBY, NICOLÁS EDUARDO
CALVO, MARTÍN EDUARDO *	MORALES, NICOLÁS EDUARDO
BUSTOS, JOSÉ MANUEL HORACIO	NEUT, FELIPE
BOZZO, JUAN ANDRÉS *	SAAVEDRA, ALDO MAXIMILIANO
BERNAL, RODRIGO CRISTOBAL *	VIAL, MANUEL AGUSTÍN
BATARCE, MATÍAS SIMÓN	VILLASECA, TOMAS VICENTE
DÍAZ, GONZALO ENRIQUE	
DONGHI, LUIS ANDRÉS	
DURÁN, GABRIEL EMILIO *	
ERENCHUN, JUAN IGNACIO	
EYZAGUIRRE, JOSÉ ANTONIO	
GALLARDO, DOMINGO ANDRÉS	
GUERRERO, ROBERTO ANTONIO *	
HEVIA, FRANCISCO JAVIER VALENTINO	
KANTOR, VICENTE CRISTIAN	
LEVICÁN, CONSTANZA GABRIEL *	
LILLO, LUIS ALBERTO	
MARTINEZ, FRANCIS HELENA *	
MELLADO, JACOB ENRIQUE *	
OGALDE, SEBASTHIAN ALEJANDRO	
PEÑA, VICENTE ALFREDO	
PERADOTTO, SEBASTIÁN IGNACIO	
QUIROZ, SEBASTIÁN	
RABBA, JAVIER EDUARDO	
RIVERA, RODRIGO IGNACIO	
SALAS, MATÍAS IGNACIO	
SCHNETTLER, JUAN PABLO	
TRONCOSO, RODRIGO FELIPE	
VILLALEIVA, CRISTIAN FELIPE	
YUSEFF, GABRIEL MATÍAS	

***Además recibieron el grado de Magister en Ciencias de la Ingeniería**

V. PROYECTOS DE INVESTIGACION

Aceleración y Validación de adquisiciones de datos de 4D flow obtenidos por resonancia magnética cardiovascular. FONDECYT. 2017 – 2020
Investigador Patrocinante: Pablo Irarrázaval

Free breathing 3D Cardiac Multiparametric Magnetic Resonance Fingerprinting. FONDECYT. 2016 – 2020
Investigador Responsable: Claudia Prieto
Coinvestigador: Pablo Irarrázaval

Identifying systemic, cellular and molecular features of metabolically normal and abnormal overweight/obesity. FONDECYT. 2017 – 2020
Coinvestigador: Pablo Irarrázaval

Multiscale Inversion of Porous Rock Physics using High-Perfomance Simulator: Bridging the Gap between Mathematics and Geophysics (MATHROCKS). Horizonte 2020, Internacional. 2017 – 2021
Investigador Asociado: Carlos Jerez

Sonification of medical data. FONDECYT. 2016 – 2020
Coinvestigador: Pablo Irarrázaval

Uncertainty Quantification and Advanced Boundary Element Methods for Electromagnetic Wave Scattering Problems. FONDECYT. 2017 – 2020
Investigador Responsable: Carlos Jerez

Cutting-edge Exoplanetary Science Using the First Generation of Chilean-funded Astronomical Optical Instrumentation. FONDECYT. 2018 – 2021
Patrocinante: Leonardo Vanzi

Enhancing motion perfomance of automated machinery in agricultural environments based on bayesian estimation approaches . FONDECYT. 2017 - 2020
Coinvestigador: Miguel Torres

The Tao Aiuc high Resolution Y band Spectrograph – TARdYS. ASTRONOMIA. 2017 - 2020
Investigador Asociado: Leonardo Vanzi

Neutrino Astrophysics in Chile. ASTRONOMIA 2017-2020 Investigador asociado: Angel Abusleme.

Centro de Investigación en Energía Solar SERC-Chile. FONDAP. 2017-2022
Investigador Asociado: Alvaro Lorca, David Watts
Investigador: Matías Negrete, Daniel Olivares

Communication and Information Research and Innovation Center (CIRIC-CHILE). Innova. 2012-2022
Investigador asociado: Sebastián Ríos

Diseño e implementación de infraestructura tecnológica para la gestión efectiva de consumos flexibles en sistemas eléctricos. FONDEF. 2018-2020
Director: Matías Negrete
Subdirector: Daniel Olivares
Investigador: Alvaro Lorca, Christian Oberli

International Center for Excellence in Solar Energy / Centro de Tecnologías para Energía Solar de Fraunhofer Chile Research (FCR-CSET). INNOVA. 2014-2023
Investigador asociado: Daniel Olivares, David Watts, Matías Negrete

Local Energy Markets for Sustainable Microgrids: Design, Modeling and Simulation. FONDECYT. 2018-2021
Investigador responsible: Daniel Olivares
Coinvestigador: Alvaro Lorca, Matías Negrete

Optimization under Uncertainty for Power System Resilience FONDECYT. 2017-2020
Investigador responsible: Alvaro Lorca

Risk Renewable Energy and Complementarity: Closing the GAP Between Portfolio Theory and Power System Planning FONDECYT. 2018-2021
Investigador responsible: David Watts
Coinvestigador: Hugh Rudnick, Matías Negrete

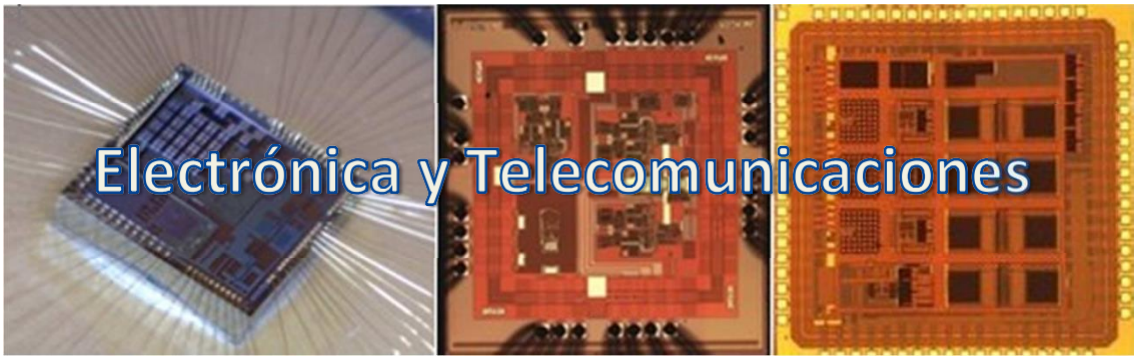

Characterizing patterns of spatio-temporal variability in snow properties trough field and remotely sensed observations. FONDECYT. 2017-2020
Coinvestigador: Christian Oberli

Experimental Particle Physics with Daya Bay, JUNO and ATLAS. FONDECYT. 2018-2021
Coinvestigador: Angel Abusleme

Experimental Particle Physics with Daya Bay, JUNO and ATLAS. FONDECYT. 2018-2021
Coinvestigador: Angel Abusleme

Modular Integrated circuits desing and its application in instrumentation circuits for particle physics experiments. FONDECYT. 2017-2021
Investigador responsible: Angel Abusleme

Enhancing motion perfomance of automated machinery in agricultural environments based on bayesian estimation approaches. FONDECYT. 2017-2020
Coinvestigador: Miguel Torres

Sistema de Análisis de Big Data en Refinerías Electrolíticas para el Mejoramiento de la Automatización y Gestión Operacional: caso Chuquicamata. FONDEF. 2017-2020
Director: Aldo Cipriano
Subdirector: Felipe Núñez

VI. ACTIVIDADES INTERNAS Y DE DIFUSION

Charla Jornadas de Orientación Académica

En el marco de las Jornadas de Orientación Académica, se realizó una charla virtual de ex alumnos los cuales nos contaron su experiencia de haber estudiado en nuestro departamento.

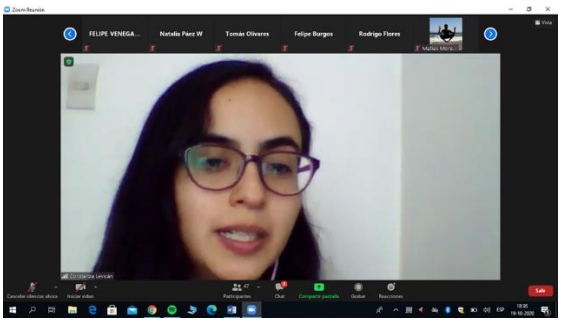

Charlas de Postgrado

Durante el 2020 se realizó el Ciclo de Charlas de los Alumnos de Postgrado, una instancia de comunicación al interior de nuestro Departamento, para mantener un feedback entre lo que se está investigando en cada área. Este año la modalidad fue online

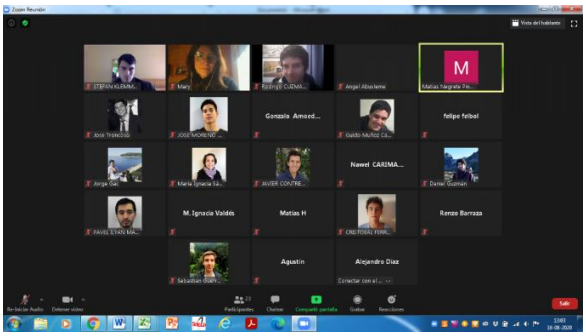

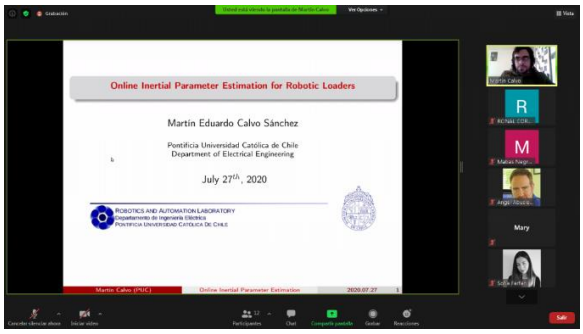

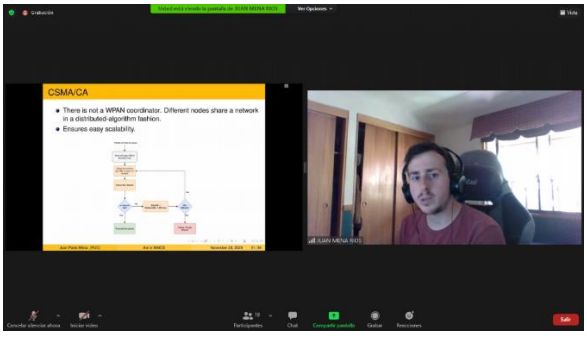

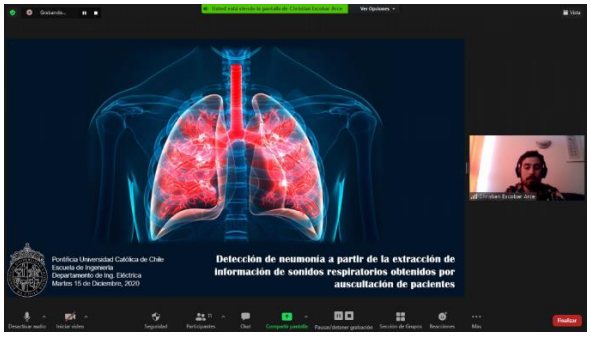

Colaboración y desarrollo de aplicaciones para enfrentar la pandemia.

El profesor Vladimir Marianov, junto a médicos y especialistas del Hospital Dr. Hernán Henríquez Aravena de Temuco y del Hospital Clínico UC, desarrollaron una aplicación gratuita que permite conocer en línea la disponibilidad de camas UTI, UCI, ventiladores invasivos y no invasivos en la red de salud pública. La app permite conocer en línea disponibilidad de camas o ventiladores para pacientes covid.

Javier Pereda grupo de académicos y alumnos de Ingeniería Eléctrica y de Mecánica y Metalúrgica de la Universidad Católica (UC), apoyados por especialistas en Infectología, desarrollaron un generador de ozono de bajo costo para eliminar la carga viral en espacios críticos. Se logró generar ozono con un equipo de bajo costo, con materiales que se encuentran en el país. El sistema cabe en una caja pequeña, que se conecta a la red eléctrica, logrando desinfectar espacios completos en solo 20 minutos de operación”

Premios

En el marco de la celebración de los 132 años de nuestra Universidad, dos académicos de nuestro departamento, Aldo Cipriano y Vladimir Marianov recibieron el grado honorífico de «Profesor Emérito»

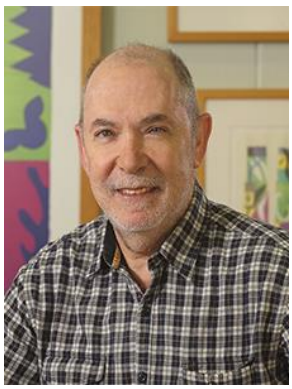

Juan Dixon Rojas, profesor de nuestro departamento recibió en premio FIDELMOV2020, reconocimiento a quienes han promovido y fomentado la electromovilidad en Chile.